Dynamic Analysis of Suspension Bridge

by

Javier Teo Han Seong

Dissertation submitted in partial fulfillment

of the requirements for the

Bachelor of Engineering (Hons)

(Mechanical Engineering)

SEPTEMBER 2011

Universiti Teknologi PETRONAS

Bandar Seri Iskandar

31750 Tronoh

Perak Darul Ridzuan

CERTIFICATION OF APPROVAL

Dynamic Analysis of Suspension Bridge

by

Javier Teo Han Seong

A project dissertation submitted to the
Mechanical Engineering Programme
Universiti Teknologi PETRONAS
in partial fulfilment of the requirement for the
BACHELOR OF ENGINEERING (Hons)
(MECHANICAL ENGINEERING)

Approved by,

_____

(Name of Main Supervisor)

UNIVERSITI TEKNOLOGI PETRONAS

TRONOH, PERAK

September 2011

CERTIFICATION OF ORIGINALITY

This is to certify that I am responsible for the work submitted in this project, that the original work is my own except as specified in the references and acknowledgements, and that the original work contained herein have not been undertaken or done by unspecified sources or persons.

_____

JAVIER TEO HAN SEONG

ABSTRACT

Any pedestrian who has crossed a suspension bridge will agree to the fact that it will move. The motion of the bridge represents the dynamic response. Typically, researchers use a combination of both analytical and experimental methods, coupled with system identification technique. However, only analytical method was implemented in this project. The suspension bridge was modeled as a fixed-fixed beam, while ignoring the effects of the hangers, bridge pylons and cable backstays. A single walking person is modeled as a single point load moving across the beam with constant speed. The critical speeds of the beam were also determined. Four different moving speeds were used.

Maximum deflection of the beam occurs when the location of the load coincides with that particular node. But at speeds near critical speeds, the maximum beam deflections do not occur at location of the load. Also, the maximum deflection undergone by a node does not occur when the load coincides with that particular node.

In future, some of the simplifications done such as ignoring should be omitted in order to produce more accurate results. A wider range of speeds should be used to further explore the effects and to determine if there is any predictable pattern of deflections in the beam model. In addition to that, the forces generated from walking should be offset to left and right of the middle of the beam or deck to imitate the alternating footsteps of a walking person. A 3D model can be created in order to study the torsional and lateral vibrations of the bridge. It can even be used to study combined vibration modes.

ACKNOWLEDGEMENTS

I would like to take this opportunity to thank several parties with regards to my Final Year Project (FYP) throughout the eight-month project period.

First of all, I would like to thank my university, Universiti Teknologi PETRONAS (UTP), for providing me with the opportunity to pursue my higher education and complete my FYP. The university provided a well-equipped computer laboratory which had allowed me to use the relevant software. Without the university facilities, I would not have been able to execute my project work.

Secondly, I would like to thank Ir Idris bin Ibrahim who is my project supervisor. I believe he has spent a lot of time and effort in advising and reviewing my progress. Despite being busy with lecturing and overseeing several other FYP students, he has been patient and committed in providing guidance for my project. As such, I would like to take this opportunity to thank him.

Thirdly, I would like to thank Mr Mohd Faizairi bin Mohd Nor, the FYP Coordinator for Mechanical Engineering Department. Without his contribution in organizing and coordinating the FYP proceedings, the project work would not have been able to proceed well.

Finally, I would like to express my gratitude to the various people who have assisted and advised me throughout the project execution time – course-mates, seniors, and friends. They provided me with both practical ideas and encouragement and it would not have been the same without their direct/indirect contributions.

TABLE OF CONTENTS

LIST OF FIGURES

LIST OF TABLES

CHAPTER 1

INTRODUCTION

1.1   Background

A bridge is basically a "structure spanning and providing passage over a river, chasm, road, or the like" [4]. It allows crossing over obstacles which are impossible or too dangerous to travel through.

There are mainly four main types of bridges whether it is for vehicular and/or pedestrian passage. The types are: beam, arch, cantilever and suspension. For this project, a suspension bridge is studied, so more attention will be given to its description.

Suspension bridges can cover a longer span than any other type of bridge. Typically they are 600 meters to 1500 meters (2000 feet to 7000 feet) long [20]. The main idea of how a suspension bridge works is the supporting of the bridge deck by cables. For a suspension bridge to function, at least two towers or piers are needed. The weight of the bridge deck is transferred to the cables, and the cables in turn transfer the load to the towers. The towers finally transfer the weight to the ground.

In the past, chains were used instead of cables to suspend the bridge deck. Nowadays, chains are no longer used. Thousands of steel wires are joined together tightly to form very strong cables which can withstand high tensile forces.

Originally, bridge decks were constructed as trusses. A truss is an arrangement of horizontal, vertical and diagonal bars which is used for supporting certain structures like roofs or bridges. The disadvantage is that trusses consume a lot of material and this adds to the overall weight. Trusses have been replaced with box-girder designs, which are basically beams with the shape of a hollow box.

1.2 Bridge Description

Following are several sketches based on photographs found on the Internet. Many details and dimensions of the bridge are still not available. The sketches are only rough estimates, and will be updated once the details are available and as the project progresses.

The figure below is a rough sketch to illustrate the bridge schematics:
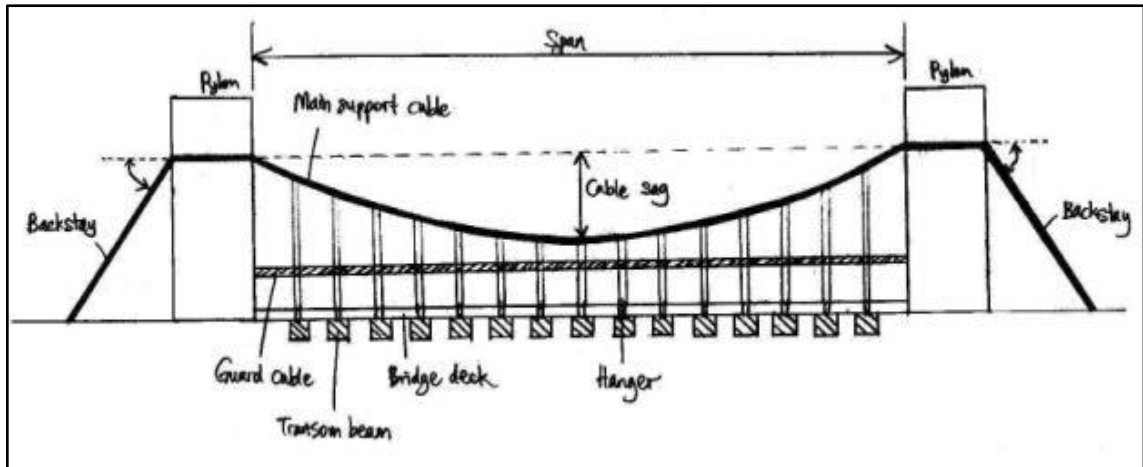
Figure 1.1: General elevation of the suspension bridge

Based on Internet searches, it seems that the bridge deck is supported by two main ways: (i) hung from the main support cable by hangers, and (ii) hung from the guard cable by smaller support wire-ropes.
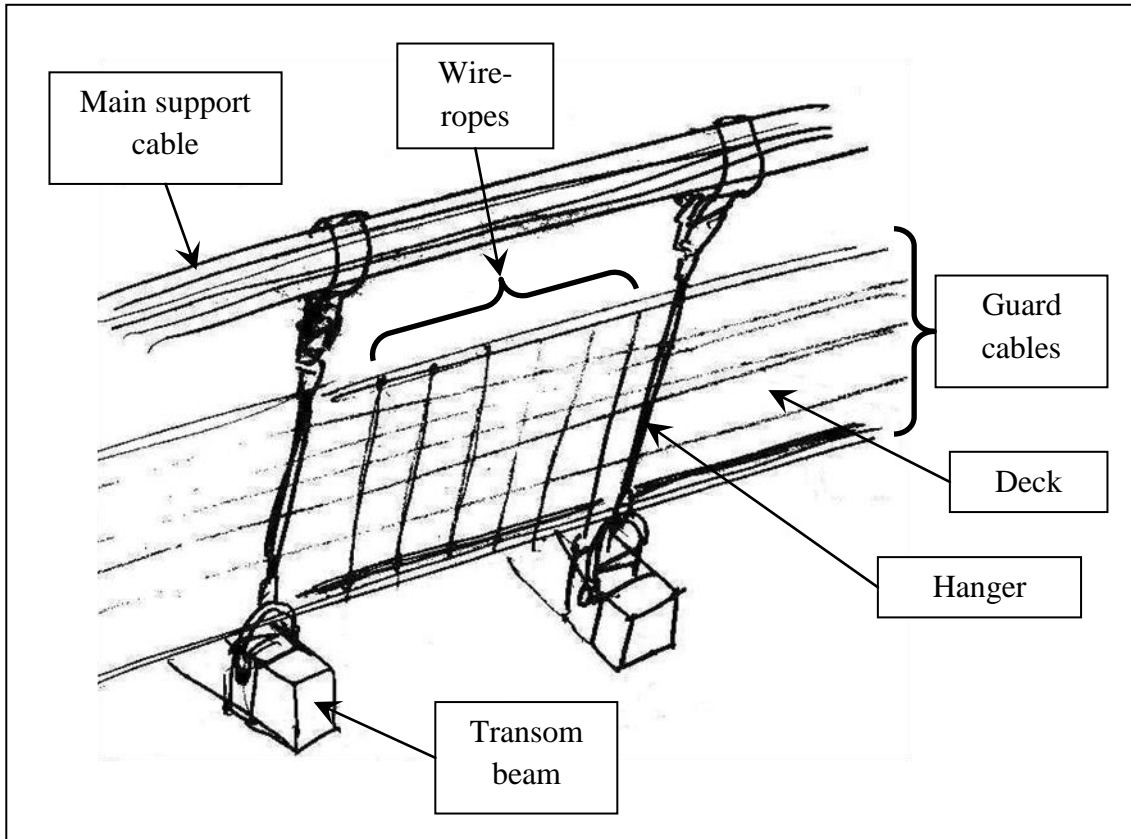
Figure 1.2: Close-up of the bridge

Hangers connect the main support cable and the transom beams underneath the deck. This is the primary way of supporting the deck weight. On the top of the deck, another cable similar to the guard cable is clamped onto the deck. Smaller support wire-ropes connect the guard cable and the deck cable, making a secondary support. The wire-ropes also form a mesh which acts as fall-protection for pedestrians who are crossing. However, for ease of analysis, it is assumed that the deck is supported by the hangers attached to main support cable alone.

1.3   Problem Statement

A suspension bridge will undergo vibrations and oscillations when pedestrians move across the bridge. For the Sunway Lagoon Theme Park suspension bridge, no research has been published so far regarding its dynamic behaviour. This necessitates the

dynamic analysis for this bridge. It is hoped that this study would be able to characterize the dynamic response and verify the safety for use of the bridge.

1.4 Objective

The objective of this Final Year Project will be to study and characterize the dynamic response of the Sunway Lagoon Theme Park suspension bridge under the influence of a uniform load (walking person). A Finite Element model is to be created in order to predict the vibration mode shapes and corresponding frequencies.

1.5 Scope of Study

In the study of the bridge, several assumptions are made in order to simplify the analysis for a Final Year Project timeframe of approximately six months:

1. Only vertical plane vibrations will be studied. Lateral and torsional vibrations are ignored. It will be assumed that (i) the design of bridge has large enough rigidity that the displacements are negligible, and (ii) the loading does not induce lateral deflections.
2. In actual situation, the suspension bridge deck has sag, but this sag will be ignored. The deck will be assumed to be horizontal and to have rigidity.
3. Wind loading is also ignored in order to simplify the analysis.
4. The bridge also has primary and secondary support methods. In order to ease the analysis, the secondary support method will be ignored.
5. This project will focus on analytical or numerical methods only. This is further explained in the Literature Review and Methodology sections.

The results to be obtained are the first four vibration mode shapes (for both vertical and torsional motions) and their corresponding frequencies, as well as the deflection or behavior of the bridge subjected to a moving load.

CHAPTER 2

LITERATURE REVIEW

Pedestrian suspension footbridges are known to shake or move noticeably when people walk across them. The vibrations or oscillations of the bridge often occur at a high enough amplitude to cause major concerns with regards to the serviceability (usability) of the bridge. A suspension bridge can respond in three ways: (i) vertical vibration, (ii) lateral vibration (side-to-side motion), or (iii) torsional vibration (twisting).

This present study is aimed at exploring and characterizing how a suspension bridge responds when a person walks across it. Specifically, vertical and torsional vibrations of the suspension bridge in Sunway Lagoon will be studied.

Typically, researchers use a combination of both analytical and experimental methods, coupled with system identification technique. Analytical (or numerical) method is an approach where a virtual or mathematical representation of a physical situation is created and used to predict the behavior of the physical situation. On the other hand, experimental method is an approach where actual testing is done on the physical situation to obtain actual data. After that, a model is created or fitted to represent the measured data accurately. However, it is generally understood or known intuitively that analytical and experimental approaches will produce different results. Therefore, researches always use system identification technique to reduce the difference or error in results. This is further explained later on. The literature review which follows is an attempt at presenting several methods of study used by various researchers.

2.1   Finite Element Method

Many times, the exact solutions for engineering problems cannot be achieved due to three main reasons. First, the governing differential equations could by themselves be too difficult to solve. Second, the boundary conditions for the problem could be too complex. Third, the initial conditions could also be too complex. Therefore, to overcome these three factors, numerical approximation is used. Finite Element (FE) method or also known as Finite Element Analysis is one numerical method which can be used to simulate real life situations in order to solve engineering problems [1].

In the complete FE analysis approach used by S. Zivanovic, A. Pavic & P. Reynolds (2007) [34], there are four main stages: (i) initial FE modeling, (ii) modal testing, (iii) manual model tuning, and (iv) automatic updating using specialist software.

In the first stage, modal properties (such as natural frequencies and mode shapes) of the footbridge can be obtained through the FE modeling. ANSYS FE codes were used to create a very detailed footbridge model.

Next, the modal properties were obtained using experimental methods in order to perform a comparison between analytically derived and experimentally obtained data. It was found that the greatest error was as high as 37% even though the Finite Element model was a very realistic one. The FE model and modal testing were used to determine the seven lowest modes of vibrations.

Based on the initial results as published by Zivanoic et al., it was made clear that modal testing is still a more reliable method for analyzing the dynamic properties of as-built structures. The natural frequencies estimated through the FE modeling were all lower than those obtained experimentally.

FE model tuning or also called FE model updating was the next stage in the study. This procedure (which is also referred to as FE model updating) is an attempt to use the best features from both the analytical and experimental model. The analytical model (FE model) was able to represent the footbridge in a very detailed manner. On the other hand, the experimental model provided more dependable modal properties of the footbridge,

including modal damping which cannot be determined through analytical approach. Horizontal longitudinal motion of the deck ends was allowed for the vertical anti-symmetric (VA) modes, and the motion was discovered to be more prominent. Springs were modeled using COMBIN14 element in ANSYS to replace free ends of the girder, and this helped to reduce the error of the FE modeling results. The stiffness of the springs was adjusted by trial-and-error until the error was minimized.

It can be concluded up until here that experimental approach provides better results compared to analytical approach. Nonetheless, this does not mean that analytical model cannot be used. Some uncertain parameters needs to be adjusted so that the model becomes more accurate and produces better results (by comparing them to the experimental results).

2.2   Discrete Parameter & Finite Element

Brownjohn (1997) used two main methods to study the vertical vibrations of a suspension bridge in Singapore. For this particular bridge that was studied, it was discovered that the most crucial component of the dynamic response was the vertical vibrations. According to Brownjohn (1997), "behaviour in the vertical plane is usually modeled with acceptable accuracy using two-dimensional models taking the deck as a beam."

The hangers were assumed to be rigid (does not deform). Due to that, the cable and deck will vibrate together. In spite of that, the cable and deck are still two different structures which have respective behaviours. Therefore, to study the how the two components affect each other, the bridge was modeled in three natures: (i) a catenary (deck has zero rigidity), (ii) a beam (cable has zero rigidity) and (iii) bridge – a combination of beams or girders suspended from a catenary cable.

The two analytical approaches used to model each of the three behaviours above were Distributed Parameter (DP) and Finite Element (FE). For DP, three continuum equations were used to represent the three bridge models. By solving those equations, the vibration

mode shapes and frequencies were obtained. On the other hand, FE involved implementation of discrete coordinates and finite elements. Using the FEA software, the modal properties were also obtained. The common assumption for each case was that the lateral and torsional characteristics are ignored by combining the total mass and stiffness characteristics into one vertical plane representation.

To double-check the accuracy of the 2D FE model, a 3D model was prepared using ANSYS and SAPIV codes. Several mode shapes were predicted using the 3D model. It was found that for vertical modes, there was little difference between the 2D and 3D models. However, the values have large errors when compared to experimentally measured values. Therefore, just as discussed in Section 2.1, experimental method provides better results than analytical method.

Next, system identification was also carried. By using original theoretical estimates and measured natural frequencies, the parameters second moment of area (I), cable modulus (E_c) and deck end rotational restraint (k_r) were adjusted. The purpose of performing system identification was to achieve a good fit between the experimental values for the first five vertical mode natural frequencies and those obtained from the 2D FE model. The least squares procedure was used.

After four iterations of adjustments, the results of the analytical models were observed to be more accurate. Other than that, the researcher concluded that the DP model was very advantageous for predicting first vertical symmetric frequency (f_{VS1}) and first vertical asymmetric frequency (f_{VA1}) only. Based on the research results, it was concluded that the cable axial stiffness is most important for the first symmetric mode (VS1). Besides this, the other modes were like a beam with partially fixed ends. This was shown through the FE system identification sensitivity matrix.

2.3   Peak Picking & Enhanced Frequency Domain Decomposition

In the research paper produced by Gentile & Gallino (2008), two methods were also presented and compared. Morca suspension bridge was the bridge studied. It is a historic bridge in Varallo Sesia located in northern Italy.

First of all, ambient vibration data is obtained by measuring the deflections of the bridge under loading (pedestrians and wind loads). Natural loading was preferred because of several reasons: (i) no equipment is required, (ii) the natural loading will always be present, and (iii) it is least invasive or obstructive to the usual use of the bridge.

Then, two methods are used to extract the modal parameters from the measured data: Peak Picking (PP) and Enhanced Frequency Domain Decomposition (EFDD). The three parameters determined through the operational modal analyses were natural frequencies, mode shapes and modal damping ratios.

For both these methods, evaluation of spectral matrix in the frequency domain was carried out. In addition to that, the techniques were based on the assumption that the inputs causing motion have white noise characteristics in the frequency range of interest. In other words, that the input loadings are not exciting the system at a specific frequency. As a result, the frequencies related with any significant response reflect only the modal characteristics of the structure.

Later, using the results as well as system identification technique, a 3D FE model of the bridge is created. This system identification technique was implemented to determine the dependence of the natural frequencies of the FE model on the unknown structural parameters. Differences between experimental and theoretical modal response can also be reduced through the same method.

Final part of the study was a live-load static test carried out by placing a vehicle at certain positions along the bridge. The static tests were done to achieve further confirmation of the dynamics-based model updating.

It was discovered that both analysis methods (PP and EFDD) provide similar results. Five normal vibration modes were found at five different frequencies. Several

assumptions were made regarding the actual design of the bridge in order to simplify the 3D modeling work. Certain parameters such as elastic modulus (E), shear modulus (G) and vertical moment of inertia (I) were updated to enhance the match between experimental and theoretical natural frequencies. The 3D model is found to fit experimentally identified modal parameters as well as the results of live load testing (measured data). From these findings, the model is considered to represent the actual bridge with high accuracy and thus, can be used for long-term monitoring of the bridge.

CHAPTER 3

METHODOLOGY

In order to perform the dynamic analysis, an approach which combines manual calculations and ANSYS modeling was used. Firstly, the equations of motion for the model of the bridge were derived in order to calculate the modal frequencies and predict the deflections of the beam under Free Vibrations.

After that, the model was created using ANSYS. Modal Analysis was done to extract the modal frequencies. The results were compared with the results obtained through manual calculations. Once the results were verified to be similar, this would signify the accuracy of the ANSYS model.

Thus, the study can be continued with Forced Vibration analysis. In this Chapter, the steps and derivation of equations are listed out in detail.

3.1   Relevant Equations for Manual Calculations

3.1.1   Force Function

A suitable force function is required to model the footsteps of a person while he or she is walking across a bridge. A force function was adopted from the research by Ricciardelli and Briatico (2011), as defined below:

$$F(x,t) = F_0 \sin(\omega t)\delta(x - vt) \tag{3.1}$$

where F_0 = amplitude of the force

ω = frequency of the force

δ = Dirac delta function

As seen in Eq (3.1), there is a Dirac delta function term to represent magnitude of the harmonic force at location x = vt, where v is the constant velocity of the walking person. The function above was adopted because it can represent the load generated by a walking person which in real life, varies with respect to location and time.

Typically for a leisurely stroll, a person would walk at a rate of two steps per second. Since, two steps are taken per second, the magnitude of the force from the person's static weight is assumed to vary sinusoidally at frequency, ω of 2Hz. The person's weight is taken to be 65kg or 637.65N. Also, the walking person was assumed to be a single point load moving at constant velocity. The speeds used are listed in a later section.

3.1.2 Equations of Motion for Transverse Vibrations of a Beam [12]

$$\frac{\delta}{\delta x^2}\left[EI(x)\frac{\delta^2 w}{\delta x^2}(x,t)\right] + \rho A(x)\frac{\delta^2 w}{\delta t^2}(x,t) = f(x,t) \tag{3.2}$$

Eq (3.2) above is the equation of motion for non-uniform beams; the second moment of area, I is a function of the location along the length of the bridge, x. For beams with uniform cross-sectional area, the equation reduces to:

$$EI\frac{\delta^4 w}{\delta x^4}(x,t) + \rho A(x)\frac{\delta^2 w}{\delta t^2}(x,t) = f(x,t) \tag{3.3}$$

Eqs (3.4), (3.5) and (3.6) below outline the modal frequency, ω_n; mode shape, W_n and response, w_n of a fixed-fixed beam. (The bridge is has fixed supports at both ends. Thus, a fixed-fixed beam is used to represent it.)

$$\omega_n = (\beta_n l)^2 \sqrt{\frac{EI}{\rho A l^4}} \tag{3.4}$$

$$W_n = C_{1n}[(\cos\beta_n x - \cosh\beta_n x) - \sigma_n(\sin\beta_n x - \sinh\beta_n x)] \tag{3.5}$$

$$w_n(x,t) = \sum_{n=1}^{4} W_n(x)[A_n \cos\omega_n t + B_n \sin\omega_n t] \tag{3.6}$$

The constants β_n needed for the two equations above are listed in Table 4.1 below.

Table 3.1: Constants

$\beta_1 l = 4.730041$	$\beta_1 = 0.011051$
$\beta_2 l = 7.853205$	$\beta_2 = 0.018349$
$\beta_3 l = 10.995608$	$\beta_3 = 0.025691$
$\beta_4 l = 14.137165$	$\beta_4 = 0.033018$

(where l = 428m)

Now that the general equations have already been defined, the next step would be to determine the initial conditions of the beam. The beam representing the bridge deck is assumed to be made of chengal wood. The properties and parameters are listed as below:

Table 3.2: Beam parameters

Dimensions:	Length, l	428 m
	Width, b	1.8 m
	Thickness, h	0.05 m
Modulus of elasticity, E		19,600 MPa
Density, ρ		980 kg/m^3
Second moment of area, I= $\frac{1}{12}bh^3$		18.75$\times$10^{-6} m^4

The initial conditions of the beam were unknown, so assumptions were made based on estimation:

a) The beam length is 428m

b) At 0m and 428m, deflection is 0

c) At the middle (214m), the deflection is 1.5m

So with the above assumption, the initial conditions were determined to be:

$$w_0 = 0.00032753x^2 - 0.014017x \tag{3.7}$$

$$\dot{w}_0 = 0.000655604x - 0.014017 \tag{3.8}$$

where w_0 refers to the initial deflection, and $\dot{w}_0$ refers to initial velocity of the beam at locations x.

By using the appropriate constants from Table 3.1, as well as Eqs (3.7) and (3.8), the Fourier coefficients were obtained as below:

Table 3.3: Fourier coefficients

$A_1 = 1.8478$	$B_1 = 0.4622$
$A_2 = 0.1453$	$B_2 = 0.3675$
$A_3 = 0.3157$	$B_3 = 0.0490$
$A_4 = 0.0516$	$B_4 = 0.0726$

For complete derivation for all the equations above, please refer to the Appendix (Section A).

3.2   Manual Calculation of Modal Frequencies

Using the values listed in Tables 3.1 and 3.2 above, the values are substituted into Eq (3.4) to determine the modal frequencies for the first four vibration modes. The results obtained are listed out in Section 4.1. After completing the calculation of modal frequencies manually, the next step was to compare the results with ANSYS modeling results.

3.3   ANSYS Modeling

3.3.1   Creating a 2D Model

First of all, "BEAM3" element was defined as the type of element to be used when the beam is sub-divided into smaller elements. Then, the Material Properties were defined: (i) Modulus of elasticity = 1.96 x 10^{10} Pa, (ii) Poisson ratio = 0.3 (typical value for most materials), and (iii) Density = 980 kg/m^3. Constants for the BEAM3 element were defined as well: (i) Cross-sectional area = 0.09m, (ii) Second moment of area = 1.875 x 10^{-5} m^4, and (iii) Height = 0.05m.

Since the 428m long beam is to be divided into 30 elements of equal length, there will be 31 nodes. The 31 nodes are created and labeled first. After that, Node 1 is joined to Node 2 to create Element 1, Node 2 to Node 3 to create Element 2 and so on. This procedure is repeated until all 30 elements were created.

The codes used are outlined in detail in the Appendix (Section C.1).

3.3.2 Modal Analysis

In the Solution stage, Modal Analysis was set as the analysis type. Next, the method of Modal Analysis needs to be selected. In order to compare the different methods, two methods were used – Block Lanczos and Subspace. Next, the number of modes to extract was set to 4. After that, boundary conditions need to be set. Since the beam has fixed support at both ends, all degrees of freedom (DOFs) for displacements – Ux, Uy and RotZ – were set to zero. This was done for both Points 1 and 2. With that, the setup is done, and the solution is started.

The results of this analysis in ANSYS are outlined in more detail in Section 4.x. It must be highlighted that at this present point, the results obtained through ANSYS agree well with manual calculations results. It can thus be concluded that the ANSYS model is accurate enough. This also signified the completion of Free Vibration analysis, and justified that the study can proceed into Forced Vibration analysis.

3.4   Transient Analysis – Modeling of Moving Point Load

3.4.1 Critical Speeds

The critical speeds of the load need to be considered when performing Transient Analysis. The equation used was (Forbes, 2008) [5]:

$$c_{cr} = \frac{\omega_n L}{\pi} \tag{3.9}$$

where L is the beam length and ω_n is the modal frequency. (n = 1, 2, 3…)

The critical speeds for the first four modes of vibrations are listed in Section 4.3.1.

3.4.2   Finite Element Analysis Approach

As explained earlier (in Section 3.1.1), the walking person is modeled as a single point load moving at constant speed. Finite Element Analysis approach was adopted. The equations of motion involved for Finite Element Analysis, modeling the moving point load, as well as the ANSYS codes used for the Transient Analysis are derived in much greater detail in the Appendix (Section C.3).

For this Transient Analysis, four different speeds for the load were used: 0.09m/s, 0.18m/s, 0.45m/s and 0.90m/s to test the behavior of the fixed-fixed beam when subjected to a load moving at speeds near to the critical speeds.

Using the various speeds, 1000 time-steps were used to perform the analysis. Basically, the time required for the load to completely traverse the entire length of the beam will be different, depending on the speed. The total time required for each respective speed will be divided into 1000 time-steps, and the nodal forces and deflections will be analyzed at each of these time-steps.

After the solution was done, the nodal deflections at quarter-span, mid-span and three-quarter-span were plotted against time. The deformed shapes of the beam with the load at roughly quarter-span, mid-span and three-quarter-span were also plotted.

3.5 Project Planning

3.5.1 FYP I (MAB4012) – May 2011 Semester

Table 3.4: Timeline for FYP I

WEEK	3	4	5	6	7	8	9	10	11	12	13	14
Obtain list and compile summary of references	▓											
Select bridge and obtain information of bridge	▓	▓										
Research and background study												
Search for journal papers			▓	▓	▓							
Study on developing force function						▓	▓	▓				
Study on developing Finite Element model									▓	▓		
Study on simulation setup and executing											▓	▓
Prepare Extended Proposal Defense		▓	▓									
Submit Extended Proposal Defense				▓	▓							
Prepare for Proposal Defense					▓							
Proposal Defense						▓	▓					
Prepare Interim Draft Report									▓	▓		
Submit Interim Draft Report											▓	
Submit Interim Report												▓

3.5.2 FYP II (MAB 4024) – September 2011 Semester

Table 3.5: Timeline for FYP II

WEEK	1	2	3	4	5	6	7	8	9	10	11	12	13	14
Research work														
Develop actual force function	▓	▓												
Develop equivalent beam			▓	▓										
Create Finite Element model					▓									
Obtain vibration mode shapes and frequencies						▓								
Results verification (comparison with other research papers)							▓	▓	▓					
Prepare Progress Report						▓	▓							
Submit Progress Report								▓						
Prepare Draft Report										▓	▓			
Submit Draft Report												▓		
Prepare Dissertation											▓	▓		
Submit Dissertation													▓	
Prepare Technical Paper											▓	▓		
Submit Technical Paper													▓	

Oral Presentation														▨
Submit Project Dissertation (hardbound) **After Oral Presentation														

3.5.3 Milestones

The milestones to be reached in order to fulfill the objective of the project are listed in the table below:

Table 3.6: Milestones for FYPII

| WEEK	1	2	3	4	5	6	7	8	9
Develop actual force function		▨							
Develop equivalent beam				▨					
Create Finite Element model					▨				
Obtain vibration mode shapes and frequencies						▨			
Results verification (comparison with other research papers)									▨

CHAPTER 4

RESULTS AND DISCUSSION

4.1   Manually Calculated Modal Frequencies

As stated in Section 3.2, the values listed in Tables 3.1 and 3.2 were substituted into Eq (3.4) in order to calculate the modal frequencies, ω_n. The calculated values are tabulated below:

Table 4.1: Modal frequencies

Mode, n	Natural frequency, ω_n (Hz)
1	0.001257
2	0.003454
3	0.006780
4	0.011205

Also, the mode shapes W_n were also determined and plotted using MATLAB. The following Figures show the first four vibration mode shapes for the beam.
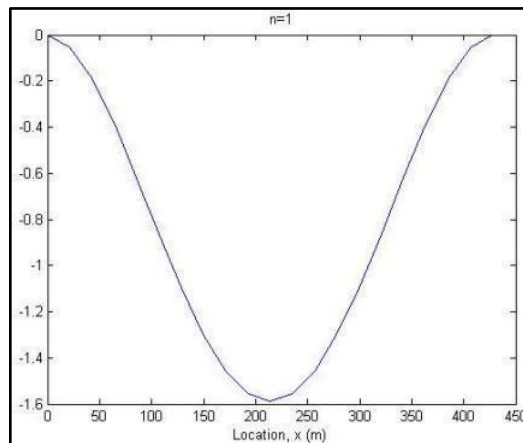
Figure 4.1: Mode shape plot (W) for n=1
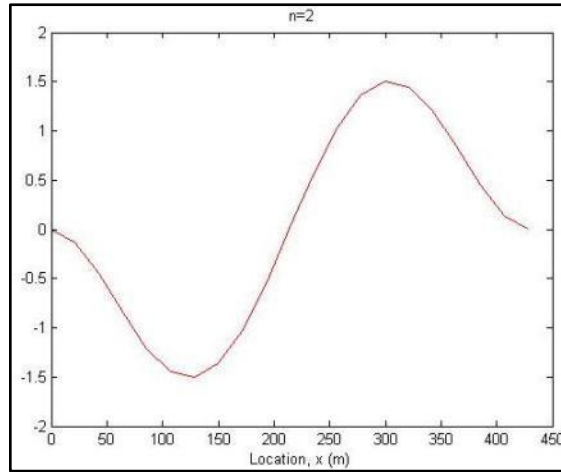
Figure 4.2: Mode shape plot (W) for n=2

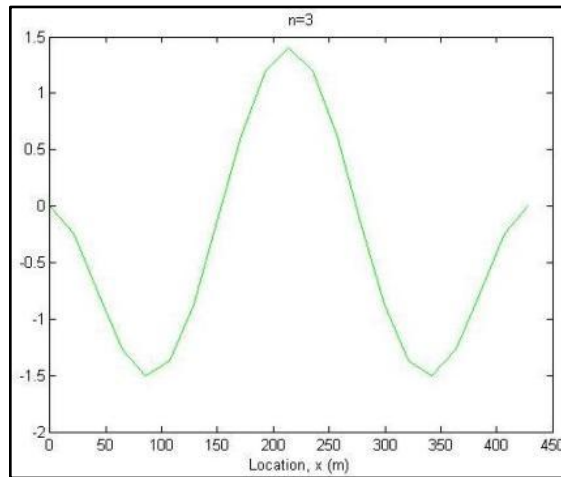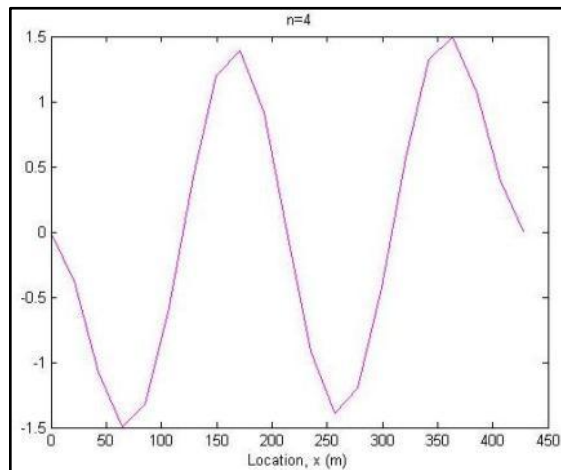*Figure 4.3: Mode shape plot (W) for n=3*

Figure 4.4: Mode shape plot (W) for n=4

21

4.2 Verification of Results with Modal Analysis in ANSYS

After performing the manual calculations of the natural frequencies for the free vibrations of the fixed-fixed beam model, the results were compared with the values.

The table below is a summary of the results obtained through ANSYS, compared to the results obtained through manual calculation:

Table 4.2: Comparison of Results

| Mode, n | Natural frequency, ω_n (Hz) | | | Percentage difference | |
| | Manual calculation | ANSYS | | Block Lanczos method | Subspace method |
		Block Lanczos method	Subspace method		
1	0.001257	0.001255	0.03110	0.002%	2374%
2	0.003454	0.003459	0.03999	0.145%	1058%
3	0.006780	0.006781	0.04995	0.015%	636.7%
4	0.011205	0.011209	0.06103	0.036%	444.7%

From the compiled results, it is very clear that one set of the ANSYS results agree well with the manual calculation, which is the set computed using the Block Lanczos method. It can also be observed that the Subspace method does not produce very accurate results, with percentage error of up to more than 2000%. With that, it was established that BEAM3 element can produce accurate results. It was also decided that any Modal analyses will be done with Block Lanczos method.
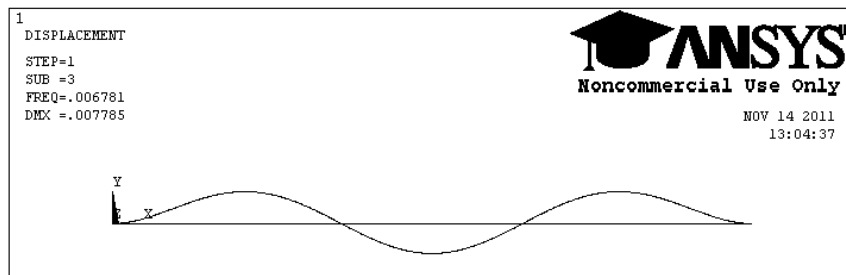
The Figures below show the deformed shapes for the first four modes of vibrations:
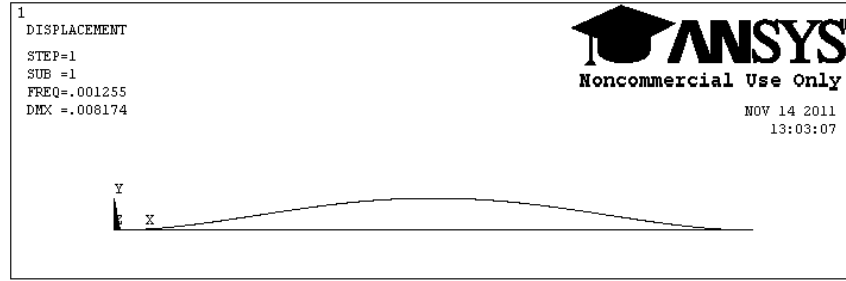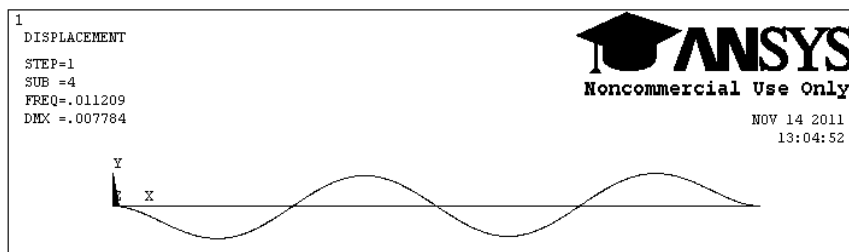
Figure 4.5: First mode shape
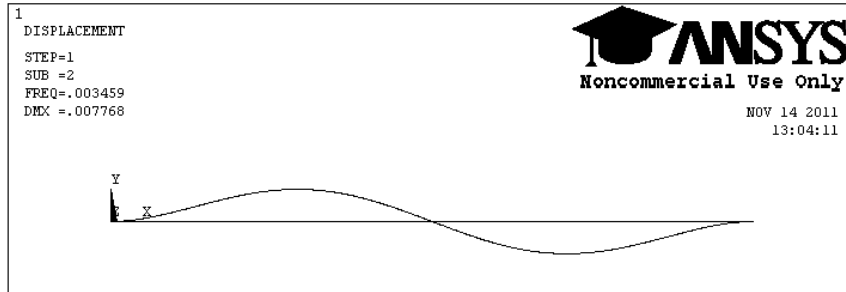
Figure 4.6: Second mode shape

Figure 4.7: Third mode shape

Figure 4.8: Fourth mode shape

It can be observed that the shapes are the same as the ones plotted using MATLAB. Therefore, it is verified that the 2D model in ANSYS is able to yield accurate results. With that, the Free Vibrations Analysis is concluded and Forced Vibration Analysis can commence.

4.3   Results of Transient Analysis – Modeling of Moving Point Load

4.3.1   Listing of Critical Speeds

Using Eq (3.9), the critical speeds are calculated and tabulated:

Table 4.3: Critical speeds for beam length, L = 428m

n	Modal frequency, ω_n (Hz)	Critical speed, c_{cr} (m/s)
1	0.001257	0.171
2	0.003454	0.471
3	0.006780	0.924
4	0.011205	1.527

4.3.2   Finite Element Analysis in ANSYS

Again, as already mentioned in Section 3.1.1, the detailed codes used are available in the Appendix (Section B). Following are the results and discussions for the behavior of the beam under the four proposed speeds (0.09m/s, 0.18m/s, 0.45m/s and 0.90m/s), as per Section 3.4.2.
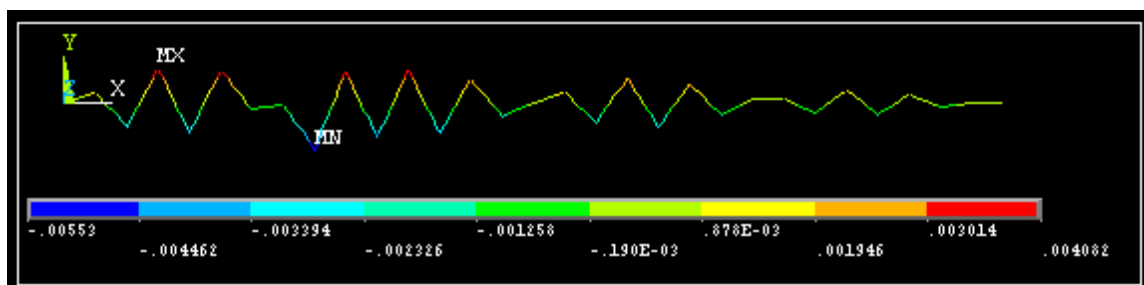
Velocity, V = 0.09m/s

Figure 4.9: Deflection shape of beam with load at quarter-span (V = 0.09m/s)

It can be observed that relatively larger magnitude of deflections occurs within the vicinity of the left side of the beam, which is where the load is located for the current time-step displayed in Figure 4.9 above.
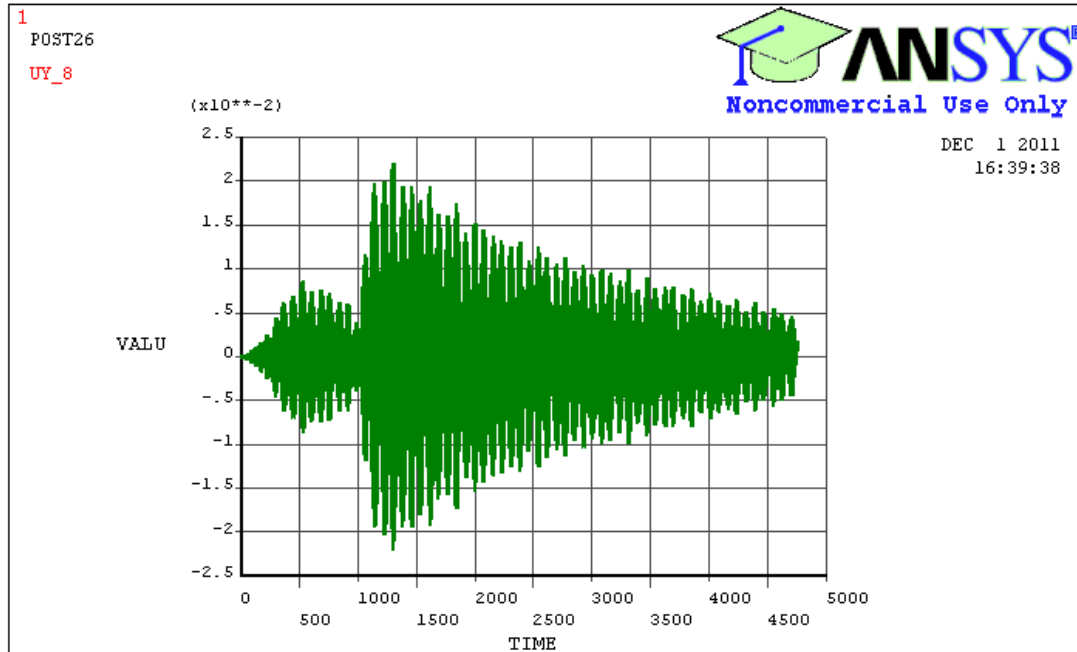
Figure 4.10: Deflections at quarter-span (Node 8, V = 0.09m/s)

When the deflections at quarter-span (Node 8) were plotted with respect to time as shown in Figure 4.10 above, it can be observed that the peak deflection occurs at about 1300 seconds. This translates to the load being at location 1300s × 0.09m/s = 117m, which is about quarter-span.

Based on this and the previous observations, it can be concluded that the maximum deflection will occur at where the load is located.
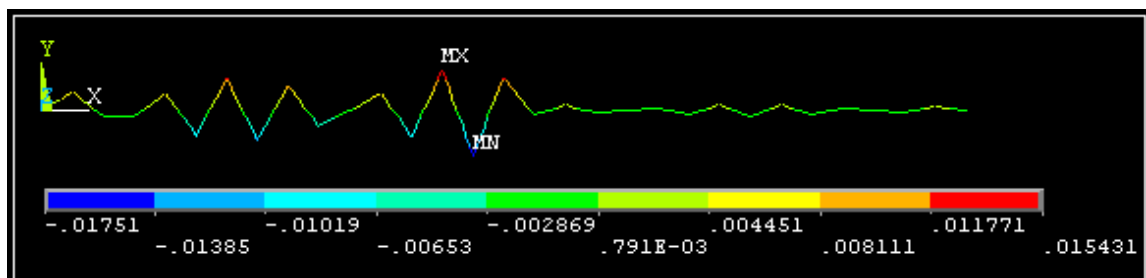

Figure 4.11: Deflection shape of beam with load at mid-span (V = 0.09m/s)

From the Figure above, a similar outcome is observed. Relatively larger magnitude of deflections occurs within the vicinity of where the load is at.
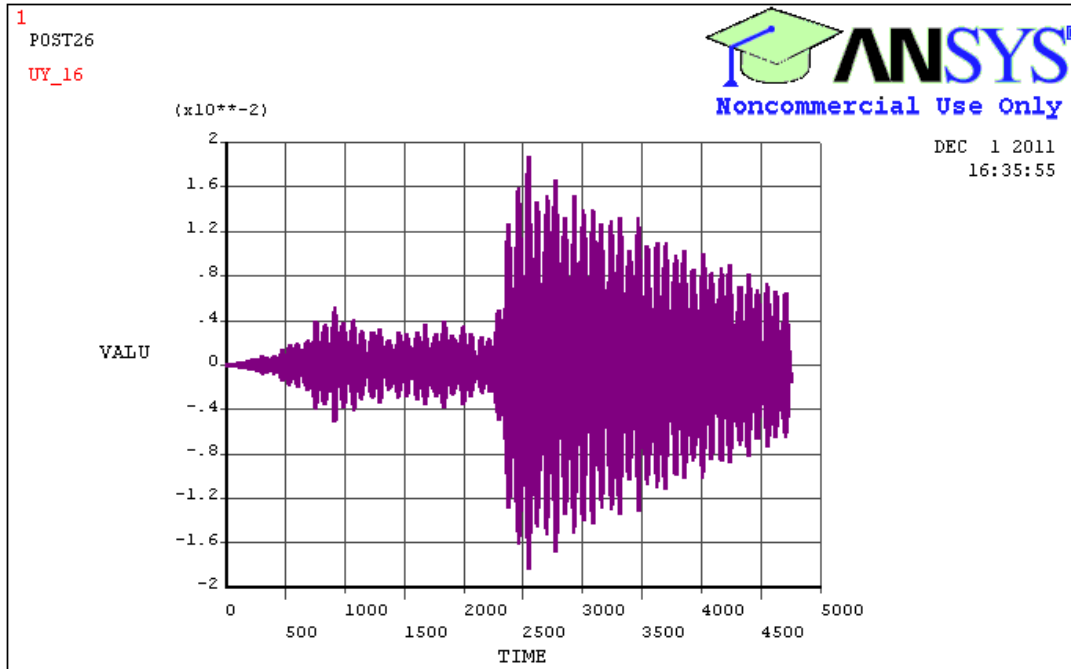
Figure 4.12: Deflections at mid-span (Node 16, V = 0.09m/s)

To verify the earlier conclusions made for the deflections at Node 8, the same will be done for Node 16. Maximum deflection at Node 16 occurs at time 2500 seconds. That translates to the load located at point 2500s × 0.09m/s = 225m, which is roughly mid-span. Thus, the same conclusion can be drawn from results for Node 16 – maximum deflections occur at where the load is located.
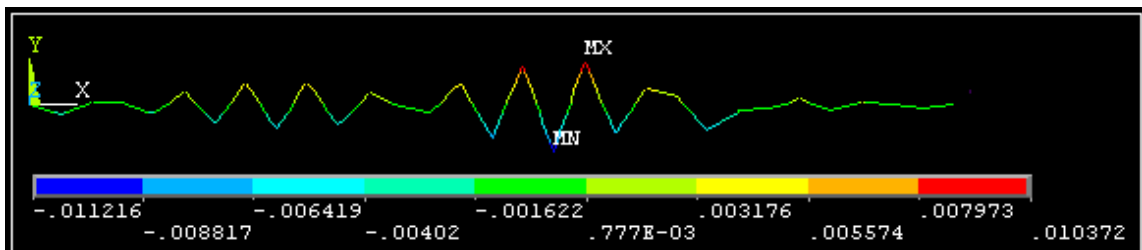

Figure 4.13: Deflection shape of beam with load at three-quarter-span (V = 0.09m/s)

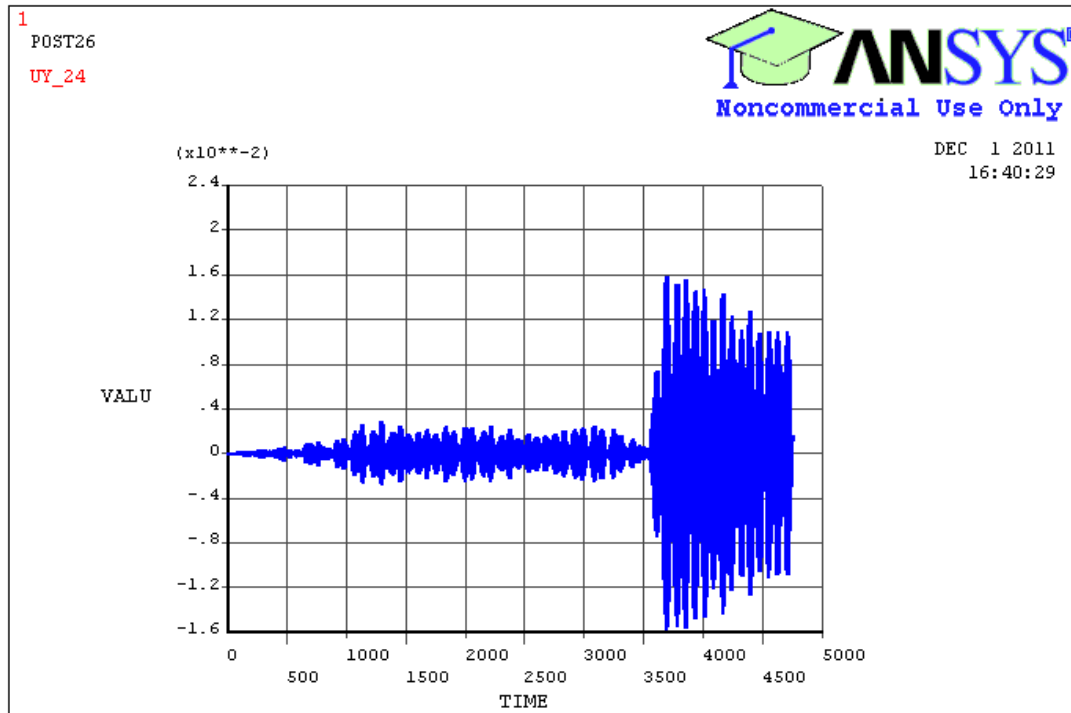The pattern is repeated for when the load is located at three-quarter span.

26

Figure 4.14: Deflections at three-quarter-span (Node 24, V = 0.09m/s)

Peak deflection for Node 24 occurs at time = 3700s. This translates to the load being at location 3700s × 0.09m/s = 333m, which is roughly three-quarter span.

For all three plots of Deflections vs Time for the three locations (Nodes 8, 16 and 24), there is another pattern which can be observed. There are three noticeable patterns of motion. Firstly, the deflections were small in the beginning. Secondly, there will be a jump in the deflections. After reaching the peak, the deflections will gradually decay.

The small deflections in the beginning show that other sections of the beam were still excited, even though the moving load is still located towards the left end of the beam (before reaching quarter-span/mid-span/three-quarter-span).

As discussed earlier, peak deflection occurs where the load is located. Therefore, there will be a drastic jump in the magnitude of deflection (about 8 to 10 times). But after the load moves past a particular node, the deflection at that node will begin to decay gradually because the source of excitation (the moving load) has moved away from the node.

According to American Association of State Highway and Transportation Officials (AASHTO)'s Standard Specifications, the safety limit for pedestrian-use bridges is L/1000. Thus, safety limit for this beam model is 0.428/1000 = 0.428m. The maximum deflection of the beam subjected to a 65kg load moving at speed of 0.09m/s is about 0.018m. Safety factor is 0.428/0.018 = 23.8. This indicates that the beam is safe for one person walking across it at speed of 0.09m/s.

Velocity, V = 0.18m/s

The simulation is repeated with V = 0.18m/s, which is near to the first mode critical speed ($c_{cr}^{(1)}$ = 0.171m/s). Thus, it was expected that the pattern of deflection would be different than that of a velocity far away from the critical speed. Using V = 0.18m/s, the beam exhibits a different pattern of deflection as shown in the Figures which follow.
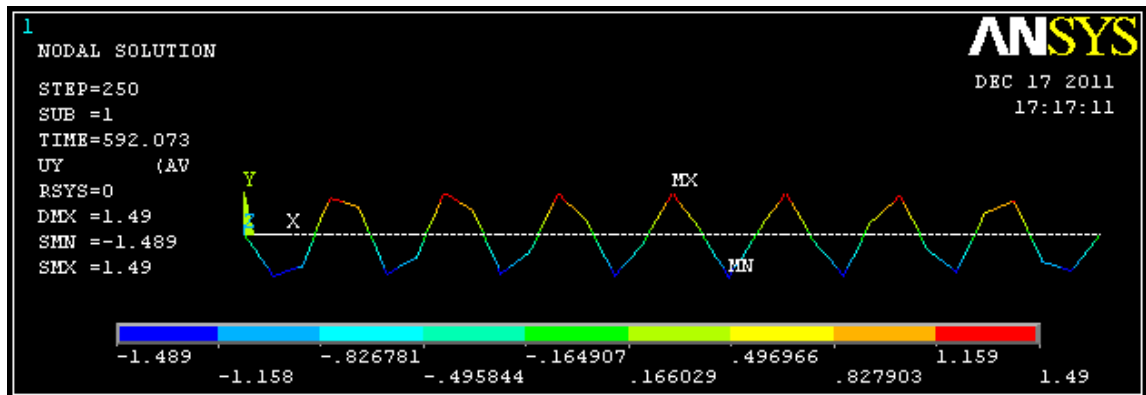
Figure 4.15: Deflection shape of beam with load at quarter-span (V = 0.18m/s)

Based on the Figure above, the maximum deflections occur near the middle of the beam even though the load is at quarter-span for that time-step. This is not the same behavior as that of the previous iteration (with V = 0.09m/s).

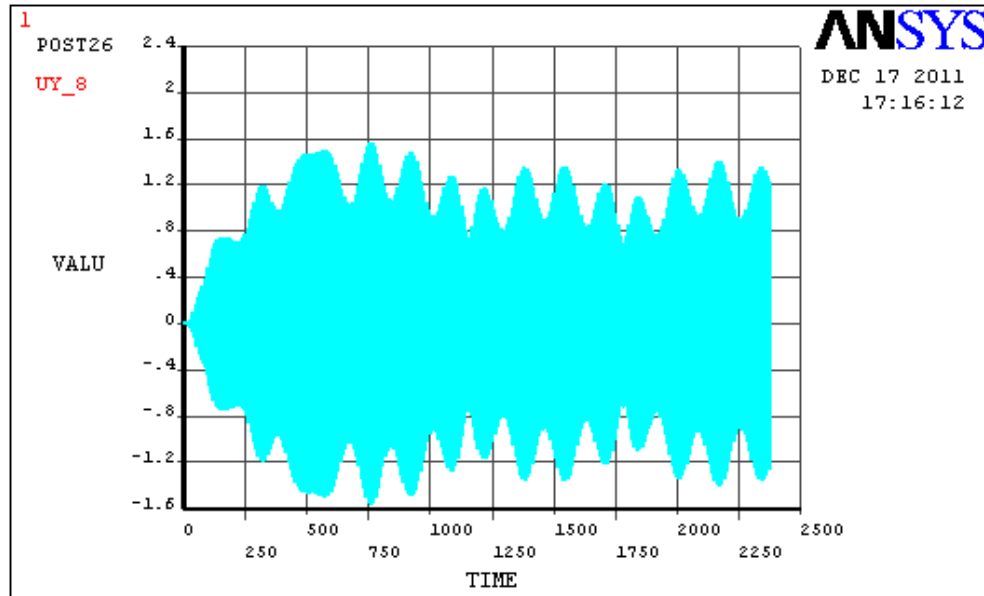*Figure 4.16: Deflections at quarter-span (Node 6, V = 0.18m/s)*

The pattern of nodal deflection is different than the previous iteration. No distinct peak is noticeable for Node 8 deflections.
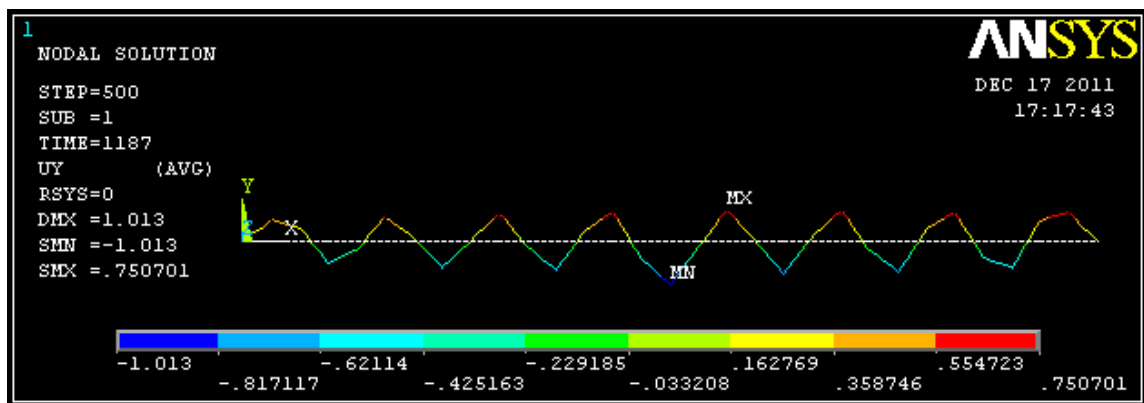
Figure 4.17: Deflection shape of beam with load at mid-span (V = 0.18m/s)

However, when the load is at mid-span, the maximum deflections occur within the vicinity of the middle of the beam.

Figure 4.18: Deflections at mid-span (Node 16, V = 0.18m/s)

For the nodal deflection at Node 16, there is no obvious peak in the deflections. The pattern of nodal deflection is the same as the one exhibited at Node 8.

Figure 4.19: Deflection shape of beam with load at three-quarter-span (V = 0.18m/s)

Maximum deflections occur near the region of three-quarter-span which coincides with position of the moving load.
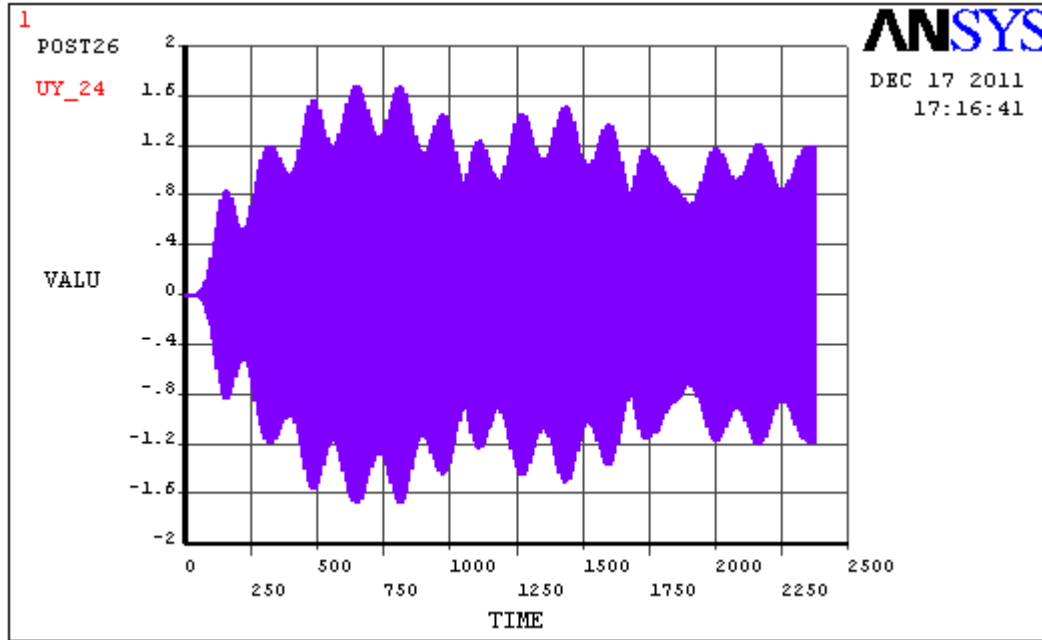
Figure 4.20: Deflections at three-quarter-span (Node 24, V = 0.18m/s)

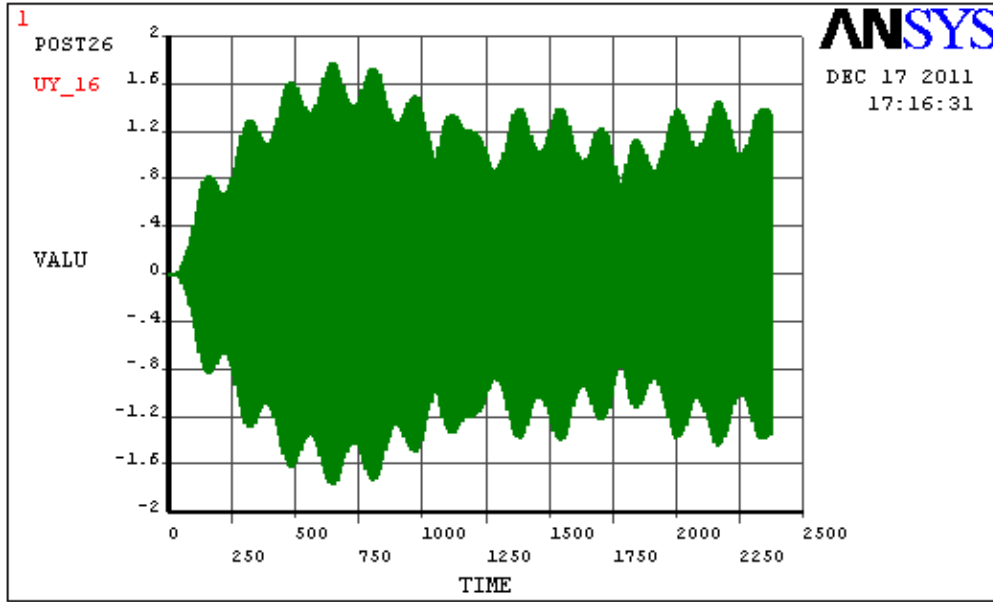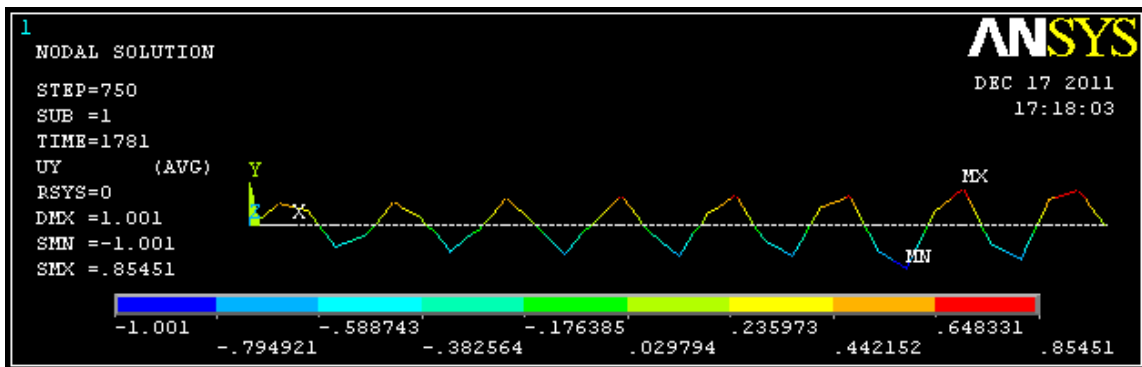The pattern of nodal deflection persists for Node 24. There is also no distinct peak in deflection.

For V = 0.09m/s, it was observed that maximum nodal deflection will occur when the load coincides with that particular node. Therefore, the deflections for this current iteration (V = 0.18m/s) are tabulated for comparison to see if there is a similarity.

Table 4.4: Magnitude of nodal deflections at specific time-steps (V = 0.18m/s)

Time-step	Location of load	Maximum deflection (m)	Deflection at node which coincides with load location (m)
250	Quarter-span	1.490	1.445
500	Mid-span	1.013	0.853
750	Three-quarter-span	1.001	0.690

Safety limit is determined to be 0.428m/1.490m = 0.287. This clearly shows that the beam no longer complies with safety limits when the load traverses across the beam at 0.09m/s.

The results obtained thus far are most likely inaccurate because the stiffness estimated for this beam is too low compared to the actual bridge. For simplicity of analysis, the effects of bridge hangers and other supports were ignored. This causes the overall stiffness of the beam model to be much lower than the actual stiffness of the physical bridge.

In addition, based on the Table above, it is noted that the maximum deflection does not occur at the node which coincides with the load location. This is probably due to a different behavior of the beam when the velocity of the moving load is close to the critical speed. In order to verify this, the simulation is re-run with several other velocities. The results are displayed and analyzed in the following sections.

Velocity, V = 0.45m/s

In this iteration, V is taken to be 0.45m/s. It is noted that this velocity is also close to the critical speed for the second vibration mode ($c_{cr}^{(2)}$ = 0.471m/s).

Figure 4.21: Deflection shape of beam with load at quarter-span (V = 0.45m/s)

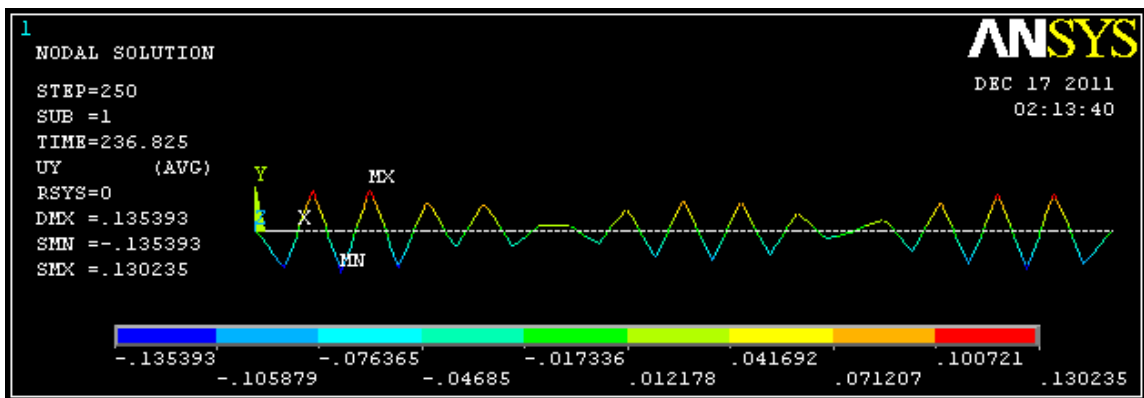In this time-step, the load is at quarter-span but maximum deflection occurs at roughly one-fifth distance instead of the predicted location of quarter-span.
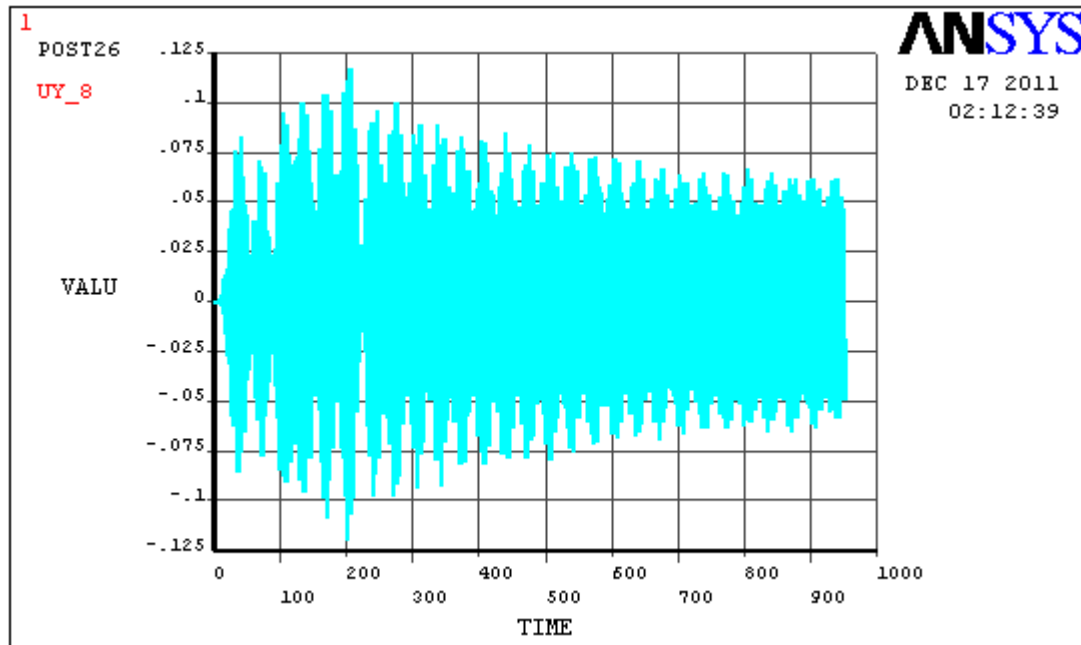
Figure 4.22: Deflections at quarter-span (Node 8, V = 0.45m/s)

For V = 0.45m/s, the nodal deflection shape for Node 8 is similar to the one with V = 0.09m/s. The deflection peaks at a certain point, and then becomes smaller after that point. From the Figure above, the peak occurs at roughly 200s × 0.45m/s = 90m, which is actually at one-fifth length instead of quarter-span. Also in the Figure, it can be seen that there is a sudden drop in deflection as well, which is estimated to occur at 235s × 0.45m/s = 106m. This location corresponds to quarter-span position, but the deflection is very small; about 0.05m.
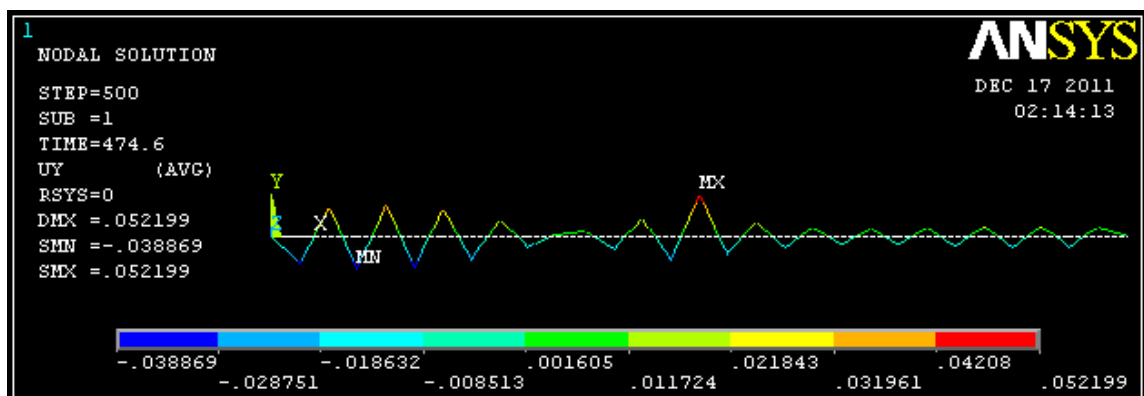
Figure 4.23: Deflection shape of beam with load at mid-span (V = 0.45m/s)

For this time-step, the load is at mid-span and maximum deflection does occur near to the middle of the beam model.
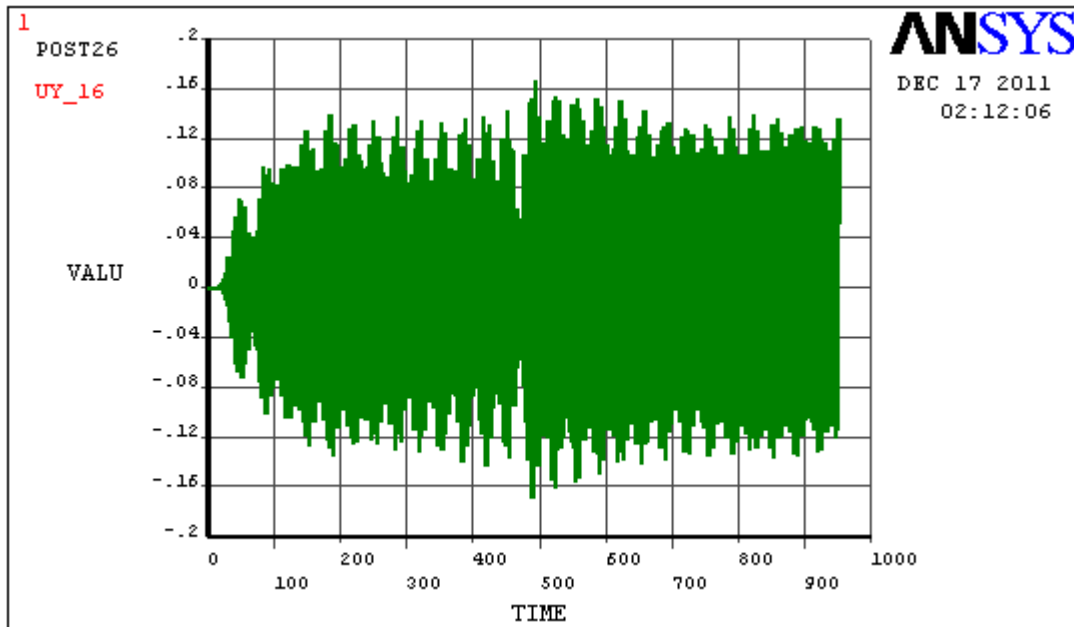
Figure 4.24: Deflections at mid-span (Node 16, V = 0.45m/s)

For Node 16, the deflection peaks at roughly 495s × 0.45m/s = 223m, which is actually slightly after mid-span position. There is also a sudden drop in deflection as well, similar to what is seen for Node 8. It is estimated to occur at 475s × 0.45m/s = 214m. This location is exactly mid-span position, and the deflection is about 0.05m which happens to be the maximum deflection for that particular time-step (when load location coincides with Node 16).
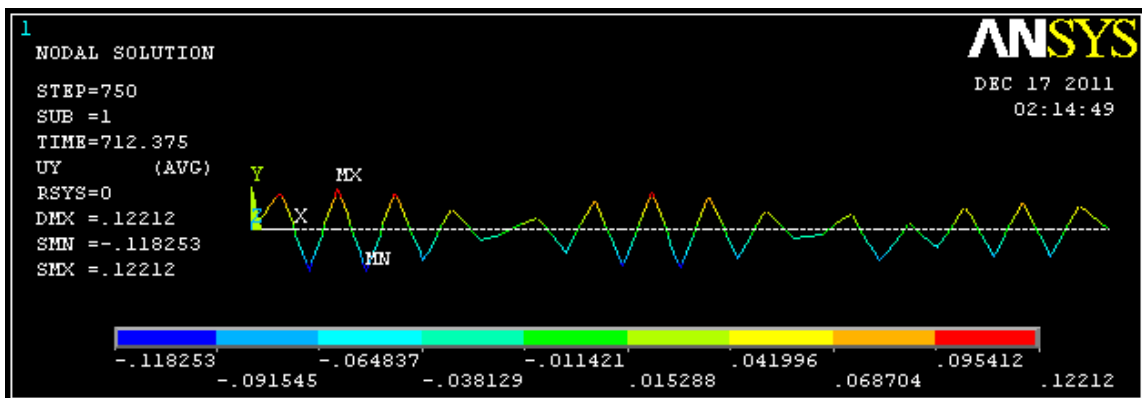
Figure 4.25: Deflection shape of beam with load at three-quarter-span (V = 0.45m/s)

The maximum deflection again occurs at roughly one-fifth location instead of at three-quarter-span position.
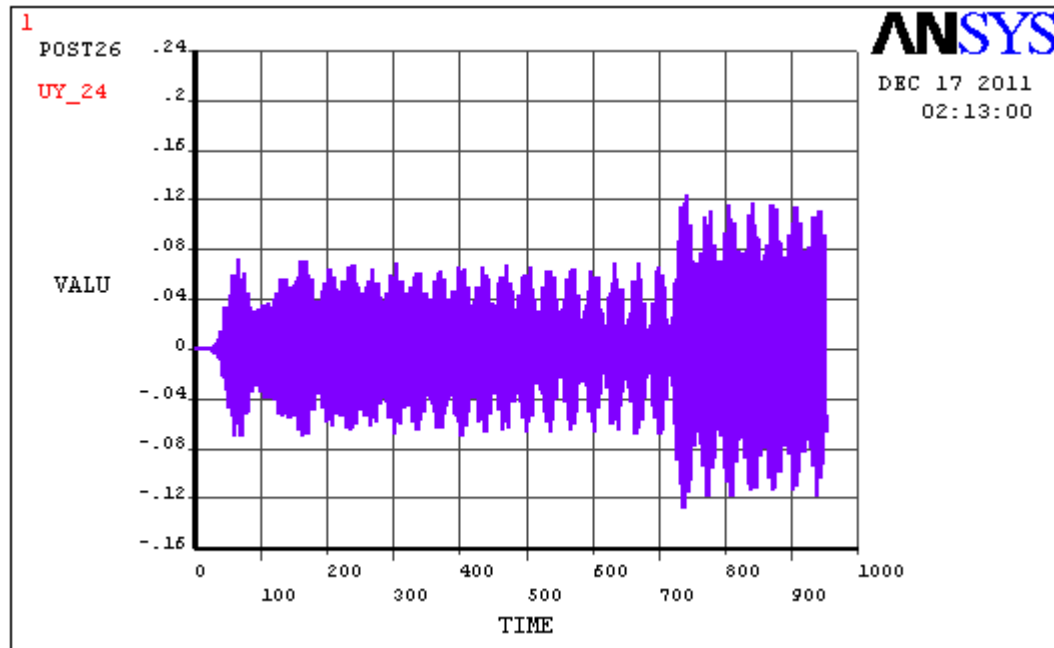
Figure 4.26: Deflections at three-quarter-span (Node 24, V = 0.45m/s)

For Node 24, the nodal deflection pattern is similar to that of V = 0.09m/s. The earlier deflections are lower, and then there is a jump. The jump occurs at $740s \times 0.45m/s =$ 333m, which is after three-quarter-span location with magnitude of about 0.12m. Analyzing the sudden drop point at $720s \times 0.45m/s = 324m$, which is almost three-quarter-span location but the deflection is roughly 0.02m only.

From observations of the nodal deflections, it is noticed that when the load position coincides with a particular node, the deflection at that particular time is small. But after the load moves away from that node, the deflection immediately rises to the maximum.

Time-step	Location of load	Maximum deflection (m)	Deflection at node which coincides with load location (m)
250	Quarter-span	0.136	0.051
500	Mid-span	0.052	0.052
750	Three-quarter-span	0.122	0.018

Like in the previous section, the maximum deflection does not occur at the location where the load is located. The safety factor is calculated as well = 0.428m/0.136m = 3.15, which is many times much smaller than the iteration with V = 0.09m/s. Nonetheless, safety factor of 3.15 is still considered safe.

Velocity V = 0.90m/s

The analysis was repeated again with load velocity of 0.90m/s to see if the model will exhibit similar pattern as the previous iteration. V is taken to be 10 times greater than the originally selected value. It is also noted that 0.90m/s is very close to the critical speed for the third vibration mode ($c_{cr}^{(3)}$ = 0.924m/s). It was expected that the pattern of deflection would be different than that of a velocity far away from the critical speed.
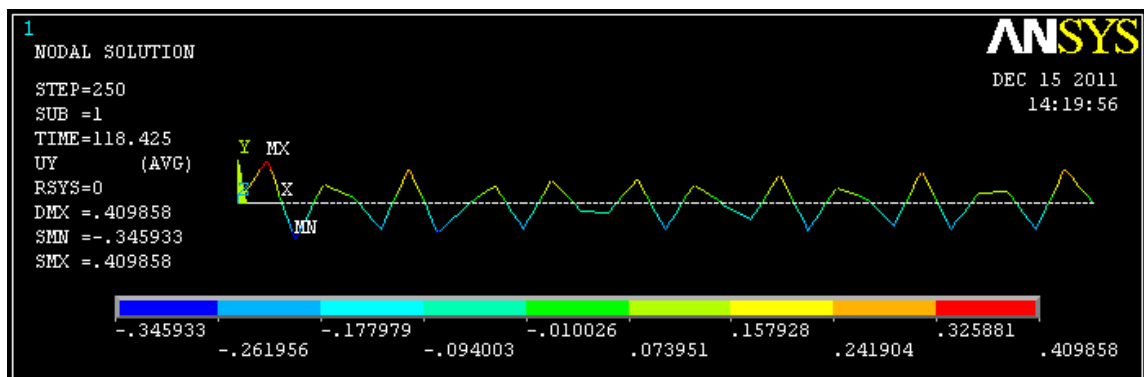
Figure 4.27: Deflection shape of beam with load at quarter-span (V = 0.90m/s)

Maximum deflection occurs at the starting end of the beam instead of at quarter-span.
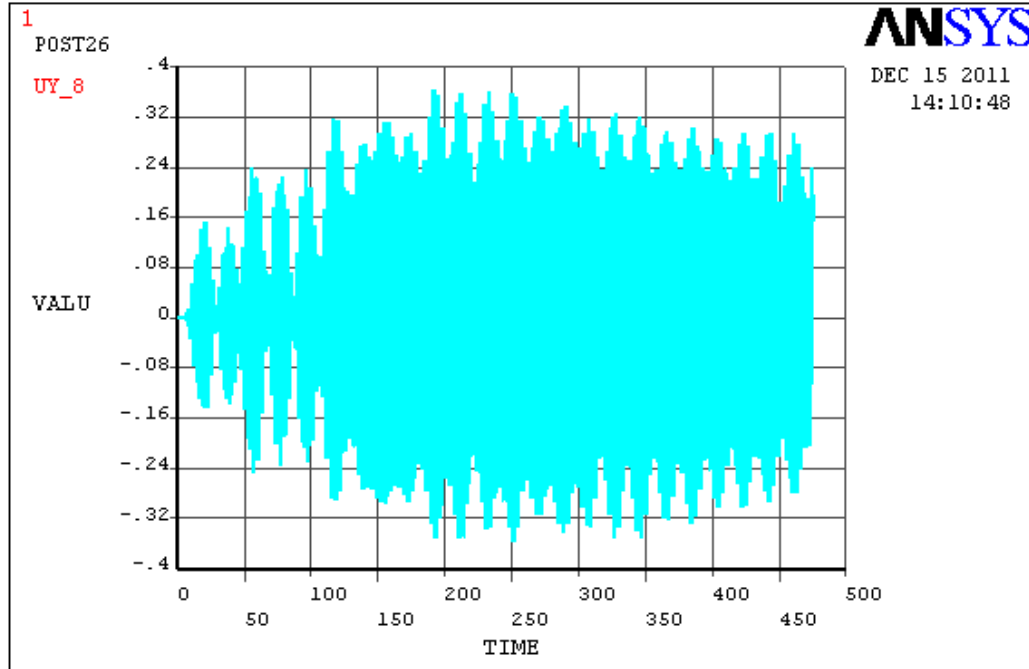
Figure 4.28: Deflections at quarter-span (Node 8, V = 0.90m/s)

The pattern of nodal deflection is different than the previous two iterations with different velocities. No distinct peak or drop is noticeable for Node 8 deflections. It can be seen that the deflections are immediately large.
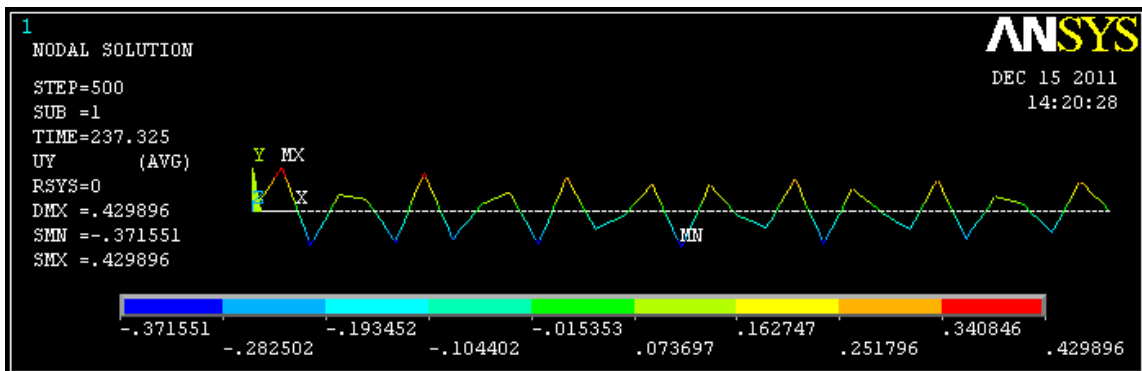
Figure 4.29: Deflection shape of beam with load at mid-span (V = 0.90m/s)

One maximum deflection occurs at roughly mid-span in this time-step.
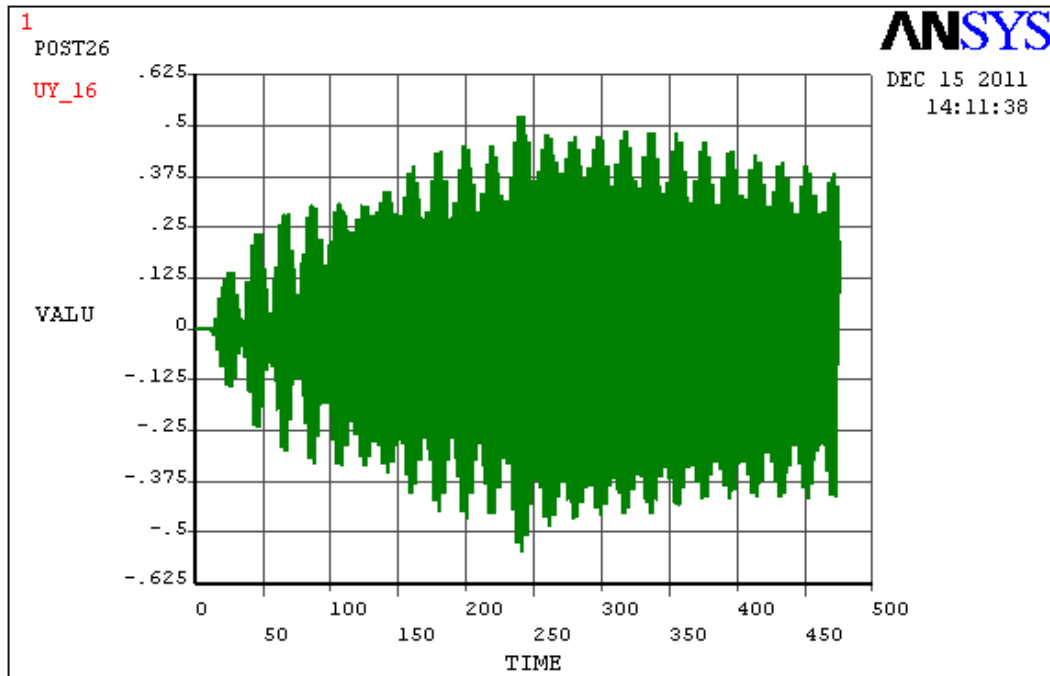
Figure 4.30: Deflections at mid-span (Node 16, V = 0.90m/s)

For Node 16, there is a more noticeable peak at roughly 240 seconds. This corresponds to the load being at location of 240s × 0.90m/s = 216m, which is mid-span. The maximum deflection experienced by Node 16 is 0.371m, which is the highest in the negative direction (refer to Figure 5.x). However, it is not the maximum in magnitude.
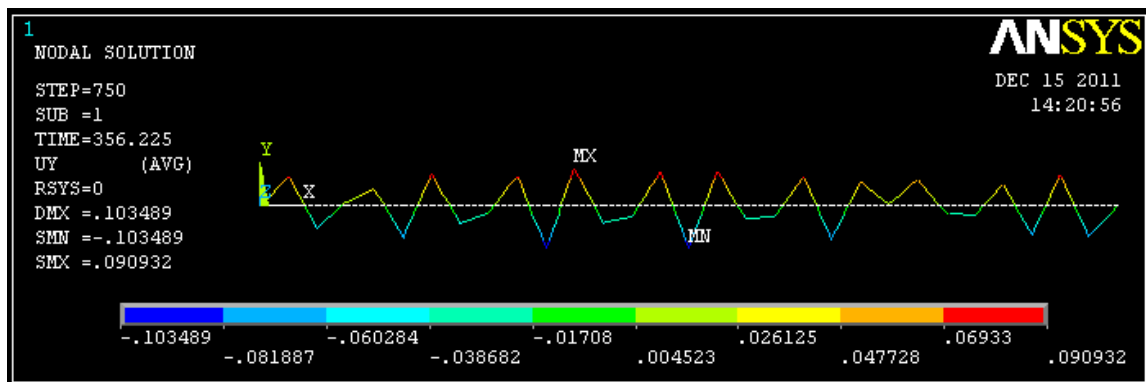
Figure 4.31: Deflection shape of beam with load at three-quarter-span (V = 0.90m/s)

Maximum deflection occurs in the vicinity of mid-span instead of three-quarter-span.
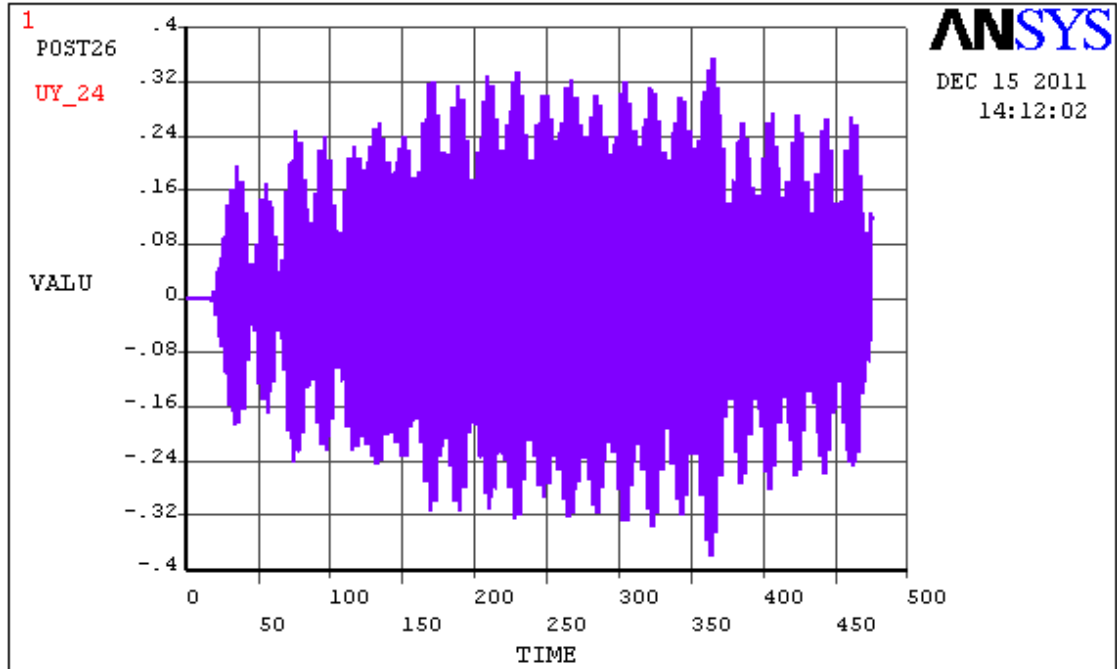
Figure 4.32: Deflections at three-quarter-span (Node 24, V = 0.90m/s)

A distinct peak is also noticeable for Node 24, which occurs at about 360 seconds. This corresponds to load location of 360s × 0.90m/s = 324m, which is roughly three-quarter-span. The maximum deflection is 0.062m.

From the Figures above, it is seen that the nodal deflections are very high throughout the entire period when the load is moving along the beam. Also, it is observed that the maximum nodal deflection does not occur when the load location coincides with the node just like the previous iterations (V = 0.18m/s and V = 0.45m/s). The Table below summarizes the deflections for clearer comparison.

Table 4.6: Magnitude of nodal deflections at specific time-steps (V = 0.90m/s)

Time-step	Location of load	Maximum deflection (m)	Deflection at node which coincides with load location (m)
250	Quarter-span	0.410	0.289
500	Mid-span	0.430	0.372
750	Three-quarter-span	0.103	0.062

From the data obtained, the overall maximum deflection is 0.524m. Safety factor is calculated to be = 0.428m/0.524m = 0.816.

Thus, the beam is not safe for use if the speed of the moving load is 0.90m/s. Again, as explained earlier, results obtained thus far are most likely inaccurate because the stiffness estimated for this beam is too low compared to the actual bridge.

4.4   Summary of Discussions

When the load moves at 0.09m/s, the maximum deflection of the beam will occur at the location of the load. For example, when the load is at mid-span, the maximum deflection will occur at the middle of the beam. Also, when a specific node is looked at closely, maximum deflection undergone by the node occurs when the location of the load coincides with that particular node. The safety factor is about 23.

For load speeds of 0.18m/s, 0.45m/s and 0.90m/s, the maximum beam deflections do not occur at location of the load. Also, the maximum deflection undergone by a node does not occur when the load coincides with that particular node. Basically, for these three speeds, the behaviour of the beam is not the same as when the speed is 0.09m/s. Sometimes, the smallest (instead of largest) nodal deflection occurs when the moving load coincides with the location of the node. Most of the time, there are no noticeable peaks in the nodal deflections. The deflections are generally much higher than the deflections experienced when subjected to load speed of 0.09m/s. These outcomes are most likely because the three speeds used are almost equal to the critical speeds of the beam.

CHAPTER 5

CONCLUSION AND RECOMMENDATIONS

5.1   Relevancy to Objectives

These completed activities have assisted in improving the understanding of the concepts and methodology relevant to the study of the dynamic response of a bridge. For example, by studying the Free Vibration response of a beam, it provided a foundation or basic understanding of the equations required to characterize the deflections. Since the free vibration study does not involve loading, it is simpler but it still provided a glimpse on how Forced Vibration study would be like. It would include some other considerations which were not involved in Free Vibration study, but this should not be too big a challenge. The Free Vibration study already helped to prepare the basic understanding needed.

Besides that, the journal papers studied presented various methodologies used to study the dynamic response of a bridge. After Finite Element method was selected as the main approach, further research was focused on how Finite Element method had been carried out, starting from the bridge modeling, to the simulation setup and to the model updating process. This helped to provide better insight on how a complete Finite Element analysis should be executed to produce the best results.

The first four vibration mode shapes (for both vertical and torsional motions) and their corresponding frequencies were calculated and verified with Finite Element modeling. Besides that, the deflection or behavior of the bridge subjected to a load moving at various speeds were studied and analyzed as well.

Based on the findings, it can be concluded that the beam model of the bridge is safe for a single person with weight 65kg, walking at constant speed of 0.09m/s, at rate of two

steps per second. However, it must also be noted that the model used is still not very accurate because the effects of other bridge structures were ignored.

The Finite Element model was created successfully as well.

5.2   Recommendations for Expansion and Continuation

For future continuation, the effect of the suspension bridge hangers, support towers/pylons and cable backstays should be included in the modeling process so that the model can be more accurate. The pylons and backstays are integral in the design of a suspension bridge, so actually ignoring the effects of these features might lead to inaccurate results. Therefore, the effects can be studied in future works to check their effects.

The speed of the load was assumed to be constant, and only four speeds were used for analysis. A wider range of speeds should be used to further explore the effects and to determine if there is any predictable pattern of deflections in the beam model.

In addition to that, it was assumed that the forces generated by the walking person were assumed to occur along a straight line in the middle of the beam. For future expansion, the load can be applied in a zigzag manner. In other words, the loads should be offset to left and right of the middle of the beam or deck to imitate the alternating footsteps of a walking person.

Besides that, the Finite Element model created in ANSYS was a 2D model. In future, a 3D model can be created in order to study the torsional and lateral vibrations of the bridge. It can even be used to study combined vibration modes.

REFERENCES

[1]   Al-Kayiem, H. (2010, January). Introduction to CAE. Tronoh, Perak, Malaysia.

[2]   Brownjohn, J. M. (1997). Vibration Characteristics of a Suspension Bridge. *Journal of Sound and Vibration* , 29-46.

[3]   Cobo del Arco, D., & Aparicio, A. (2001). Preliminary static analysis of suspension bridges. *Engineering Structures (23)* , 1096-1103.

[4]   Dictionary.com, LLC. (2011). *Bridge*. Retrieved July 8, 2011, from Dictionary.com: http://dictionary.reference.com/browse/bridge

[5]   Forbes, G. (2008, August 8). *Finite Element Modelling of Moving Loads on Structures*. Retrieved October 16, 2011, from Vibrations and Acoustics Research Group: http://www.varg.unsw.edu.au/movingload.htm

[6]   Gentile, C., & Gallino, N. (2008). Ambient vibration testing and structural evaluation of an historic suspension footbridge. *Advances in Engineering Software (39)* , 356-366.

[7]   Gonzalez, A. (2010). Vehicle-bridge dynamic interaction using finite element modelling. In I. Lipovic, *Finite element analysis* (pp. 1-26). Sciyo.

[8]   Hügül, S. (2005, August). Vibration analysis of systems subjected to moving loads by using the Finite Element method. İzmir, Turkey: Graduate School of Natural and Applied Sciences, Dokuz Eylül University.

[9]   Ljung, L. (2002). *System Identification Toolbox*. Retrieved July 10, 2011, from Dalhousie University Department of Mathematics and Statistics: http://www.mscs.dal.ca/cluster/manuals/matlab/pdf_doc/ident/ident.pdf

[10]   Moaveni, S. (2003). Example 11.8 (Section 11.6 - Examples using ANSYS). In S. Moaveni, *Finite Element Analysis: Theory and Application with ANSYS (2nd Edition)* (pp. 622-633). Singapore: Pearson Education Limited.

[11]   O'Connor, J. J., & Robertson, E. F. (2011, April). *Catenary*. Retrieved June 17, 2011, from The MacTutor History of Mathematics archive: http://www-history.mcs.st-and.ac.uk/Curves/Catenary.html

[12]   Ouyang, H. (2011). Moving-load dynamic problems: A tutorial (with a brief overview). *Mechanical Systems and Signal Processing (25)* , 2039-2060.

[13]   Ouyang, H. (2011). Moving-load dynamicproblems: A tutorial (with a brief overview). *Mechanical Systems and Signal Processing (25)* , 2039-2060.

[14]   Rainer, J. H., Pernica, G., & Allen, D. E. (1986). Dynamic Loading and Response of Footbridges. *C.S.C.E. Second International Conference on Short and Medium Span Bridges.* Ottawa, Ontario: Institute for Research in Construction, National Research Council of Canada.

[15]   Rao, S. S. (2004). Continuous Systems. In S. S. Rao, *Mechanical Vibrations (SI Edition)* (pp. 588-656). Singapore: Prentice Hall.

[16]   Rao, S. S. (2004). Free Vibrations Analysis of an Undamped System. In S. S. Rao, *Mechanical Vibrations (SI Edition)* (pp. 385-388). Singapore: Prentice-Hall.

[17]   Rao, S. S. (2007). Transverse Vibrations of Beams. In S. S. Rao, *Vibration of Continuous Systems* (pp. 387-392). Hoboken, New Jersey: John Wiley & Sons, Inc.

[18]   Ricciardelli, F., & Briatico, C. (2011). Transient Response of Supported Beams to Moving Forces with Sinusoidal Time Variation. *Journal of Engineering Mechanics (137)* , 422-430.

[19]   Rosenbrock, H. H. (1960). An automatic method for finding the greatest or least value of a function. *Comp J (3)* , 175-184.

[20]   *Suspension Bridges - Design Technology*. (n.d.). Retrieved July 8, 2011, from Design Technology: http://www.design-technology.org/suspensionbridges.htm

[21]   Tata Steel. (2011). *Box girder*. Retrieved July 8, 2011, from Tata Steel: http://www.tatasteelconstruction.com/en/reference/teaching_resources/bridges/21st_century_bridges/box_girder/

[22]   ThinkQuest. (n.d.). *Suspension Bridges*. Retrieved July 8, 2011, from Welcome to Bridges 101: http://library.thinkquest.org/J002223/types/suspension.html

[23]   Ú12105 FS ČVUT. (2004). *4.4 BEAM4 3-D Elastic Beam*. Retrieved July 14, 2011, from Mechanika: http://mechanika2.fs.cvut.cz/old/pme/examples/ansys55/html/elem_55/chapter4/ES4-4.htm

[24]   Ú12105 FS ČVUT. (2004). *4.63 SHELL63 Elastic Shell*. Retrieved July 13, 2011, from Mechanika: http://mechanika2.fs.cvut.cz/old/pme/examples/ansys55/html/elem_55/chapter4/ES4-63.htm

[25]   University of Alberta. (2001). *Harmonic Analysis of a Cantilever Beam*. Retrieved July 23, 2011, from University of Alberta - ANSYS Tutorials: http://www.mece.ualberta.ca/tutorials/ansys/IT/Harmonic/Harmonic.html

[26]   University of Alberta. (2001). *Modal Analysis of a Cantilever Beam*. Retrieved July 23, 2011, from University of Alberta - ANSYS Tutorials: http://www.mece.ualberta.ca/tutorials/ansys/IT/modal/modal.html

[27]   University of Alberta. (2001). *Transient Analysis of a Cantilever Beam*. Retrieved August 1, 2011, from University of Alberta - ANSYS Tutorials: http://www.mece.ualberta.ca/tutorials/ansys/IT/Transient/Transient.html

[28]   Wu, J.-J., Whittaker, A. R., & Cartmell, M. P. (2000). The use of finite element techniques for calculating the dynamic response of structures to moving loads. *Computers and Structures (78)* , 789-799.

[29]   Wu, S. Q., & Law, S. S. (2011). Dynamic analysis of bridge with non-Gaussian uncertainties under a moving vehicle. *Probabilistic Engineering Mechanics (26)* , 281-293.

[30]   Xia, H., Guo, W. W., Zhang, N., & Sun, G. J. (2008). Dynamic analysis of a train–bridge system under wind action. *Computers and Structures (86)* , 1845-1855.

[31]   Yau, J. D. (2009). Dynamic response analysis of suspended beams subjected to moving vehicles and multiple support excitations. *Journal of Sound and Vibration (325)* , 907-922.

[32]   Yau, J. D., & Yang, Y. B. (2008). Vibration of a suspension bridge installed with a water pipeline and subjected to moving trains. *Engineering Structures (20)* , 632-642.

[33]   Zhang, T., & Zheng, G.-T. (2010). Vibration Analysis of an Elastic Beam Subjected to a Moving Beam with Flexible Connections. *Journal of Engineering Mechanics* , 120-130.

[34]   Zivanovic, S., Pavic, A., & Reynolds, P. (2007). Finite element modeling and updating of a lively footbridge: The complete process. *Journal of Sound and Vibration (301)* , 126-145.

APPENDIX

A.　　Equations of Motion for Transverse Vibrations of a Beam [15]

The equations of motion were determined by Euler-Bernoulli's principle. A beam subjected to an external force resulting with bending is considered.
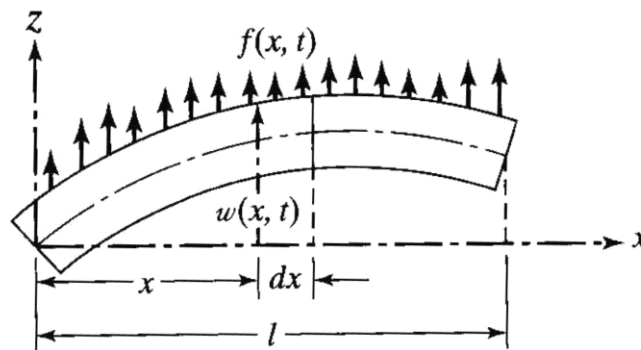
Figure A.1: Free-body diagram of a beam in bending
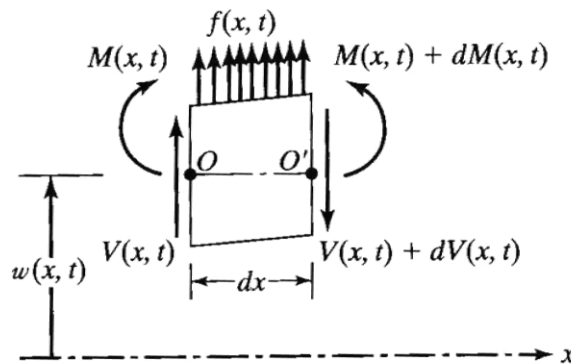
Figure A.2: Free-body diagram of an element of a beam

Let f(x,t) be the external force per unit length of the beam, V(x,t) the shear force and M(x,t) the bending moment.

Inertia force acting on an element of the beam is taken as:

$$\rho A(x) dx \frac{\delta^2 w}{\delta t^2}(x,t) \tag{A.1}$$

Referring to Figure A.1, the force equation of motion in z-direction is:

$$-(V + dV) + f(x,t)dx + V = \rho A(x)dx \frac{\delta^2 w}{\delta t^2}(x,t) \tag{A.2}$$

$$-dV + f(x,t)dx = \rho A(x)dx \frac{\delta^2 w}{\delta t^2}(x,t) \tag{A.3}$$

Moment equation of motion about y-axis, passing through point O is:

$$(M + dM) - (V + dV)dx + f(x,t)dx \frac{dx}{2} - M = 0 \tag{A.4}$$

$$dM - Vdx + dVdx = 0 \tag{A.5}$$

Take:

$$dV = \frac{\delta V}{\delta x}dx \tag{A.6}$$

$$dM = \frac{\delta M}{\delta x}dx \tag{A.7}$$

Terms involving second powers in dx are disregarded.

Substituting Eq (A.6) into Eq (A.4):

$$-\left(\frac{\delta V}{\delta x}dx\right) + f(x,t)dx = \rho A(x)dx \frac{\delta^2 w}{\delta t^2}(x,t) \tag{A.8}$$

$$-\frac{\delta V}{\delta x} + f(x,t) = \rho A(x) \frac{\delta^2 w}{\delta t^2}(x,t) \tag{A.9}$$

Substituting Eqs (A.6) and (A.7) into Eq (A.5):

$$\frac{\delta M}{\delta x} dx - V dx + \left(\frac{\delta V}{\delta x} dx\right) = 0 \tag{A.10}$$

$$\frac{\delta M}{\delta x}(x,t) - V(x,t) = 0 \tag{A.11}$$

Rearranging:

$$V(x,t) = \frac{\delta M}{\delta x}(x,t) \tag{A.12}$$

Differentiating Eq (A.12) with respect to x:

$$\frac{\delta V}{\delta x}(x,t) = \frac{\delta^2 M}{\delta x^2}(x,t) \tag{A.13}$$

Substituting Eq (A.13) into Eq (A.9):

$$-\frac{\delta^2 M}{\delta x^2}(x,t) + f(x,t) = \rho A(x)\frac{\delta^2 w}{\delta t^2}(x,t) \tag{A.14}$$

By Euler-Bernoulli theory:

$$M(x,t) = EI(x)\frac{\delta^2 w}{\delta x^2}(x,t) \tag{A.15}$$

Differentiating Eq (A.15) with respect to x twice:

$$\frac{\delta^2 M}{\delta x^2}(x,t) = \frac{\delta}{\delta x^2}\left[EI(x)\frac{\delta^2 w}{\delta x^2}(x,t)\right] \tag{A.16}$$

Substituting into Eq (A.14):

$$\frac{\delta}{\delta x^2}\left[EI(x)\frac{\delta^2 w}{\delta x^2}(x,t)\right] + \rho A(x)\frac{\delta^2 w}{\delta t^2}(x,t) = f(x,t) \tag{A.17}$$

Eq (A.17) is for non-uniform beams; the second moment of area, I is a function of the location along the length of the bridge, x. For beams with uniform cross-sectional area, the equation reduces to:

$$EI\frac{\delta^4 w}{\delta x^4}(x,t) + \rho A(x)\frac{\delta^2 w}{\delta t^2}(x,t) = f(x,t) \qquad \text{(A.18)}$$

Below are the steps in deriving the mode shape and free vibration response for a fixed-fixed beam.

For free vibrations, Eq (A.18) reduces to:

$$EI\frac{\delta^4 w}{\delta x^4}(x,t) + \rho A(x)\frac{\delta^2 w}{\delta t^2}(x,t) = 0 \qquad \text{(A.19)}$$

$$\frac{EI}{\rho A}\frac{\delta^4 w}{\delta x^4} + \frac{\delta^2 w}{\delta t^2} = 0 \qquad \text{(A.20)}$$

Take:

$$c = \sqrt{\frac{EI}{\rho A}} \qquad \text{(A.21)}$$

So, Eq (A.20) is rewritten as:

$$c^2\frac{\delta^4 w}{\delta x^4} + \frac{\delta^2 w}{\delta t^2} = 0 \qquad \text{(A.22)}$$

Let:

$$W(x)T(t) = w \qquad \text{(A.23)}$$

Substituting into Eq (A.22):

$$c^2\frac{\delta^4 (W(x)T(t))}{\delta x^4} + \frac{\delta^2 (W(x)T(t))}{\delta t^2} = 0 \qquad \text{(A.24)}$$

Separating the variables yields:

$$\frac{c^2}{W(x)}\frac{d^4W(x)}{dx^4} = -\frac{1}{T(t)}\frac{d^2T(t)}{dt^2} = a = \omega^2 \qquad \text{(A.25)}$$

Solving left hand side of Eq (A.25):

$$\frac{c^2}{W}\frac{d^4W}{dx^4} = \omega^2 \qquad \text{(A.26)}$$

$$\frac{d^4W}{dx^4} - \frac{\omega^2}{c^2}W = 0 \qquad \text{(A.27)}$$

Take:

$$\beta^4 = \frac{\omega^2}{c^2} \qquad \text{(A.28)}$$

So:

$$\frac{d^4W}{dx^4} - \beta^4 W = 0 \qquad \text{(A.29)}$$

Assume the solution for W as:

$$W = Ce^{sx} \qquad \text{(A.30)}$$

Substituting the solution into Eq (A.29):

$$\frac{d^4}{dx^4}(Ce^{sx}) - \beta^4(Ce^{sx}) = 0 \qquad \text{(A.31)}$$

$$s^4 Ce^{sx} - \beta^4(Ce^{sx}) = 0 \qquad \text{(A.32)}$$

$$(s^4 - \beta^4)(Ce^{sx}) = 0 \qquad \text{(A.33)}$$

For non-trivial solution, take $Ce^{sx} \neq 0$

Therefore:

$$(s^4 - \beta^4) = 0 \tag{A.34}$$

Solutions are:

$$s_1 = \beta \tag{A.35}$$

$$s_2 = -\beta \tag{A.36}$$

$$s_3 = i\beta \tag{A.37}$$

$$s_4 = -i\beta \tag{A.38}$$

Substituting into Eq (A.30):

$$W = C_1 e^{\beta x} + C_2 e^{-\beta x} + C_3 e^{i\beta x} C_4 e^{-i\beta x} \tag{A.39}$$

$$= C_1 \cos \beta x + C_2 \sin \beta x + C_3 \cosh \beta x + C_4 \sinh \beta x \tag{A.40}$$

Next, solving right hand side of Eq (A.25):

$$-\frac{1}{T} \frac{d^2 T}{dt^2} = \omega^2 \tag{A.41}$$

$$\frac{d^2 T}{dt^2} + \omega^2 T = 0 \tag{AA.4}$$

Assume the solution for T as:

$$T = C e^{st} \tag{A.43}$$

Substituting the solution into Eq (A.42):

$$\frac{d^2 (C e^{st})}{dt^2} + \omega^2 (C e^{st}) = 0 \tag{A.44}$$

$$s^2 C e^{st} + \omega^2 C e^{st} = 0 \tag{A.45}$$

$$(s^2 + \omega^2) C e^{st} = 0 \tag{A.46}$$

With assumption $Ce^{st} \neq 0$

So:

$$s^2 + \omega^2 = 0 \tag{A.47}$$

$$s^2 = -\omega^2 \tag{A.48}$$

$$s = \pm j\omega \tag{A.49}$$

Substituting into Eq (4.43):

$$
\begin{aligned}
T &= C_1 e^{j\omega} + C_2 e^{-j\omega} & \text{(A.50)} \\
&= C_1 \cos \omega t + C_2 \sin \omega t & \text{(A.51)} \\
&= A \cos \omega t + B \sin \omega t & \text{(A.52)}
\end{aligned}
$$

From Eq (A.28):

$$\beta^4 = \frac{\omega^2}{c^2} \tag{A.53}$$

$$\omega^2 = \beta^4 c^2 \tag{A.54}$$

Substituting Eq (A.21):

$$\omega^2 = \beta^4 \frac{EI}{\rho A} \tag{A.55}$$

$$\omega = \beta^2 \sqrt{\frac{EI}{\rho A}} = (\beta l)^2 \sqrt{\frac{EI}{\rho A l^4}} \tag{A.56}$$

For fixed-fixed beam, the boundary conditions are as below:

$$\text{Deflection} = 0; \quad W(0) = 0 \tag{A.57a}$$

$$W(l) = 0 \tag{A.57b}$$

$$\text{Slope} = 0; \qquad \frac{dW}{dx}\bigg|_{x=0} = 0 \qquad\qquad \text{(A.57c)}$$

$$\frac{dW}{dx}\bigg|_{x=l} = 0 \qquad\qquad \text{(A.57d)}$$

From Eq (A.40) earlier:

$$W = C_1 \cos \beta x + C_2 \sin \beta x + C_3 \cosh \beta x + C_4 \sinh \beta x \qquad\qquad \text{(A.58)}$$

Differentiating with respect to x:

$$\frac{dW}{dx} = \beta(-C_1 \sin \beta x + C_2 \cos \beta x + C_3 \sinh \beta x + C_4 \cosh \beta x) \qquad\qquad \text{(A.59)}$$

Using boundary condition $W(0) = 0$

$$C_1 + C_3 = 0 \qquad\qquad \text{(A.60)}$$

$$C_3 = -C_1 \qquad\qquad \text{(A.61)}$$

Using boundary condition $\frac{dW}{dx}\big|_{x=0} = 0$

$$\beta(C_2 + C_4) = 0 \qquad\qquad \text{(A.62)}$$

$$C_4 = -C_2 \qquad\qquad \text{(A.63)}$$

So now, rewriting Eqs (A.58) and (A.59)

$$W = C_1 (\cos \beta x - \cosh \beta x) + C_2 (\sin \beta x - \sinh \beta x) \qquad\qquad \text{(A.64)}$$

$$\frac{dW}{dx} = -\beta C_1 (\sin \beta x + \sinh \beta x) + \beta C_2 (\cos \beta x - \cosh \beta x) \qquad\qquad \text{(A.65)}$$

Using boundary condition $W(l) = 0$, Eq (A.64) becomes:

$$W = C_1 (\cos \beta l - \cosh \beta l) + C_2 (\sin \beta l - \sinh \beta l) = 0 \qquad\qquad \text{(A.66)}$$

Similarly, using boundary condition $\frac{dW}{dx}\big|_{x=l} = 0$, Eq (4.65) becomes:

$$\frac{dW}{dx} = -\beta C_1 \left(\sin \beta l + \sinh \beta l\right) + \beta C_2 \left(\cos \beta l - \cosh \beta l\right) = 0 \qquad \text{(A.67)}$$

Collapsing Eqs (A.66) and (A.67) into matrix form:

$$\begin{bmatrix} (\cos \beta l - \cosh \beta l) & (\sin \beta l - \sinh \beta l) \\ -(\sin \beta l + \sinh \beta l) & (\cos \beta l - \cosh \beta l) \end{bmatrix} \begin{bmatrix} C_1 \\ C_2 \end{bmatrix} = 0 \qquad \text{(A.68)}$$

For non-trivial solution, $C_1 \neq 0$, and $C_2 \neq 0$, meaning:

$$\begin{vmatrix} (\cos \beta l - \cosh \beta l) & (\sin \beta l - \sinh \beta l) \\ -(\sin \beta l + \sinh \beta l) & (\cos \beta l - \cosh \beta l) \end{vmatrix} = 0 \qquad \text{(A.69)}$$

$$(\cos \beta l - \cosh \beta l)(\cos \beta l - \cosh \beta l) + (\sin \beta l + \sinh \beta l)(\sin \beta l - \sinh \beta l) = 0$$
$$\text{(A.70)}$$

$$\cos^2 \beta l - 2 \cos \beta l \cosh \beta l + \cosh^2 \beta l + \sin^2 \beta l - \sinh^2 \beta l = 0 \qquad \text{(A.71)}$$

$$(\sin^2 \beta l + \cos^2 \beta l) + (\cosh^2 \beta l - \sinh^2 \beta l) - 2 \cos \beta l \cosh \beta l = 0 \qquad \text{(A.72)}$$

By trigonometric identities:

$$2 - 2 \cos \beta l \cosh \beta l = 0 \qquad \text{(A.73)}$$

$$\cos \beta l \cosh \beta l = 1 \qquad \text{(A.74)}$$

Since Eq (A.74) above is a transcendental equation, values for βl are determined using MATLAB. With the "fzero" function, the solutions for βl were obtained:

$$\beta_1 l = 4.7300$$

$$\beta_2 l = 7.8532$$

$$\beta_3 l = 10.9956$$

$$\beta_4 l = 14.1372$$

These values correspond with the values available in Rao [15].

Therefore, natural frequency is given as:

$$\omega_n = (\beta_n l)^2 \sqrt{\frac{EI}{\rho A l^4}} \tag{A.75}$$

Rearranging Eq (A.66) yields:

$$C_{2n} = -C_{1n}\left(\frac{\cos\beta_n l - \cosh\beta_n l}{\sin\beta_n l - \sinh\beta_n l}\right) \tag{A.76}$$

Therefore, mode shape is defined as:

$$W_n = C_{1n}[(\cos\beta_n x - \cosh\beta_n x) - \sigma_n(\sin\beta_n x - \sinh\beta_n x)] \tag{A.77}$$

where,

$$\sigma_n = \frac{\cos\beta_n l - \cosh\beta_n l}{\sin\beta_n l - \sinh\beta_n l} \tag{4.78}$$

Defined earlier in Eq (A.23), W(x)T(t) = w. Since, W in Eq (A.40) and T in Eq (A.52) were already solved, the normal mode of vibration (or the vibration response) can be written as below:

$$w_n(x,t) = \sum_{n=1}^{4} W_n(x)\left[A_n \cos\omega_n t + B_n \sin\omega_n t\right] \tag{A.79}$$

and Fourier coefficients:

$$A_n = \frac{2}{l}\int_0^l w_0 W_n\, dx \tag{A.80}$$

$$B_n = \frac{2}{\omega_n l}\int_0^l \dot{w}_0 W_n\, dx \tag{A.81}$$

The constants are summarized again in Table A.1 below:

Table A.1: Constants

$\beta_1 l = 4.730041$	$\beta_1 = 0.011051$
$\beta_2 l = 7.853205$	$\beta_2 = 0.018349$
$\beta_3 l = 10.995608$	$\beta_3 = 0.025691$
$\beta_4 l = 14.137165$	$\beta_4 = 0.033018$

(where l = 428m)

Now that the general equations have already been defined, the next step would be to determine the initial conditions of the beam. The beam representing the bridge deck is assumed to be made of chengal wood. The properties and parameters are listed as below:

Table A.2: Beam parameters

Dimensions:	Length, l	428 m
	Width, b	1.8 m
	Thickness, h	0.05 m
Modulus of elasticity, E		19,600 MPa
Density, ρ		980 kg/m^3
Second moment of area, I= $\frac{1}{12} bh^3$		18.75×10^{-6} m^4

The initial conditions of the beam were unknown, so assumptions were made based on estimation:

a) The beam length is 428m

b) At 0m and 428m, deflection is 0

c) At the middle (214m), the deflection is 1.5m

So with the above assumption, the initial conditions were determined to be:

$$w_0 = 0.00032753x^2 - 0.014017x \qquad (A.82)$$

$$\dot{w}_0 = 0.000655604x - 0.014017 \qquad (A.83)$$

where w_0 refers to the initial deflection, and $\dot{w}_0$ refers to initial velocity of the beam at locations x.

By substituting the appropriate constants from Table A.1, as well as Eqs (A.82) and (A.83) into Eqs (A.80) and (A.81), the Fourier coefficients were obtained as below:

Table A.3: Fourier coefficients

$A_1 = 1.8478$	$B_1 = 0.4622$
$A_2 = 0.1453$	$B_2 = 0.3675$
$A_3 = 0.3157$	$B_3 = 0.0490$
$A_4 = 0.0516$	$B_4 = 0.0726$

B.   Finite Element Analysis

B.1   Equations of Motion [28]

To study a structural system of certain degree of freedom, the equation of motion can be written as follows:

$$[M]\{\ddot{u}\} + [C]\{\dot{u}\} + [K]\{u\} = \{F(t)\} \tag{B.1}$$

[M] represents the global or overall mass matrix, [C] represents global damping matrix and [K] represents global stiffness matrix. $\{\ddot{u}\}$, $\{\dot{u}\}$ and $\{u\}$ are respectively acceleration, velocity and displacement for the structure. Finally, {F(t)} represents the external force function.

As mentioned previously, the person will be treated as a single point load. The magnitude can be assigned as F_0. The beam of interest is assumed to be divided into a certain number elements. As the load moves across the beam, it will pass through each element one-by-one. At the same time, the nodes of the element at which the load is at will be subjected to forces. This is illustrated as below:

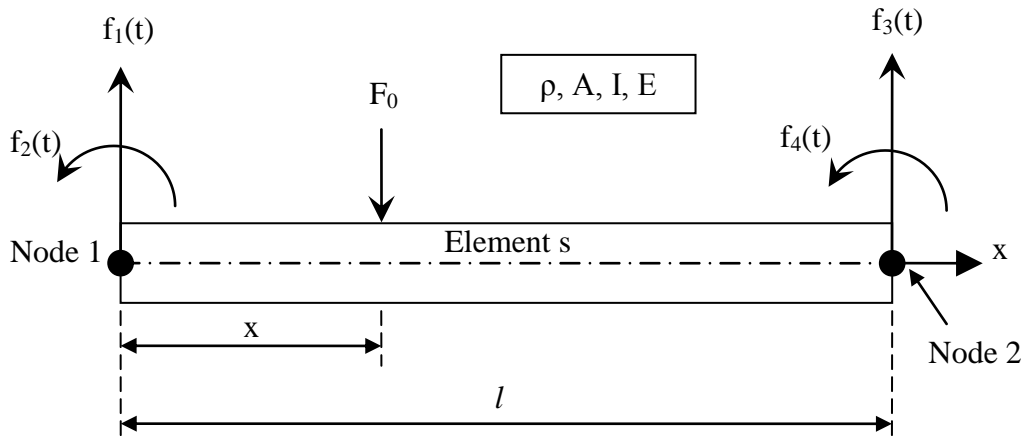*Figure B.1: Equivalent forces occurring at a particular element, s when subjected to single point load, F_0*

Each element is given a number (s) with each element being of length *l*. *x* indicates the distance of the point load with respect to the starting node of that element.

The force function can be represented as a force vector:

$$\{f^{(s)}(t)\} = \left| f_1^{(s)}(t) f_2^{(s)}(t) f_3^{(s)}(t) f_4^{(s)}(t) \right|^T = F_0\{N\} \tag{B.2}$$

$\{N\}$ is a vector representing shape functions [28].

$$\{N\} = \lfloor N_1 N_2 N_3 N_4 \rfloor^T \tag{B.3}$$

$$N_1 = 1 - 3\xi^2 + 2\xi^3 \tag{B.4}$$

$$N_2 = (\xi - 2\xi^2 + \xi^3)l \tag{B.5}$$

$$N_3 = 3\xi^2 - 2\xi^3 \tag{B.6}$$

$$N_4 = (-\xi^2 + \xi^3)l \tag{B.7}$$

$$\xi = {x}/{l} \tag{B.8}$$

To expand this elemental equation to cover the entire length of the beam, the equations need to be slightly modified to accommodate all elements.

Let the load be moving at speed V, and number of time steps be set as m. Considering a specified time interval Δt, the total time will be:

$$t_{max} = m\Delta t \tag{B.9}$$

The position of the load is first determined using:

$$x_p(t) = Vt = Vr\Delta t \tag{B.10}$$

where r is any integer between 1 and m.

After that, it can be determined which the load is located at by using $x_p(t)$, as shown below:

$$\text{Element number, s} = (\text{Truncate or Integer part of } \frac{x_p(t)}{l}) + 1 \tag{B.11}$$

The formula for ξ will also be modified to accommodate for the other elements depending on location of the load $(x_p(t))$.

$$\xi = \frac{x_p(t) - (s-1)l}{l} \tag{B.12}$$

With that, the nodal forces and moments can then be calculated using the equations below:

$$F_{t=r\Delta t}^{s} = F_0 N_1 \tag{B.13}$$

$$F_{t=r\Delta t}^{s+1} = F_0 N_3 \tag{B.14}$$

$$M_{t=r\Delta t}^{s} = F_0 N_2 \tag{B.15}$$

$$M_{t=r\Delta t}^{s+1} = F_0 N_4 \tag{B.16}$$

It must also be noted that the shape functions N cited here are specific to beam elements only. The appropriate shape functions should be applied for other element types (such as bar element or torsion element).

B.2   Nodal Forces Resulting From a Moving Point Load

To illustrate how the nodal forces vary, a plot is done using Microsoft Excel.

Using the 428m-long beam, the first four elements are studied more closely. Since the 428m beam is divided into 30 equal-length beams, each beam is 428/30 = 14.267m long. It is arbitrarily assumed that 10 time-steps are required to completely traverse one element.

Assuming velocity of load as 0.09m/s, total time required, ttotal = 428m/0.09m/s = 4755.556s. Total steps, m = 10 steps × 30 elements = 300 time-steps. So, time interval per step, Δt = 4755.556s/300 steps = 15.852s.

Therefore, using values of V = 0.09m/s, l = 14.267m, Δt = 15.852s, elements s = 1, 2, 3 and 4, the forces for Nodes 1, 2, 3, 4 and 5 were calculated, and plotted in the following Figure.
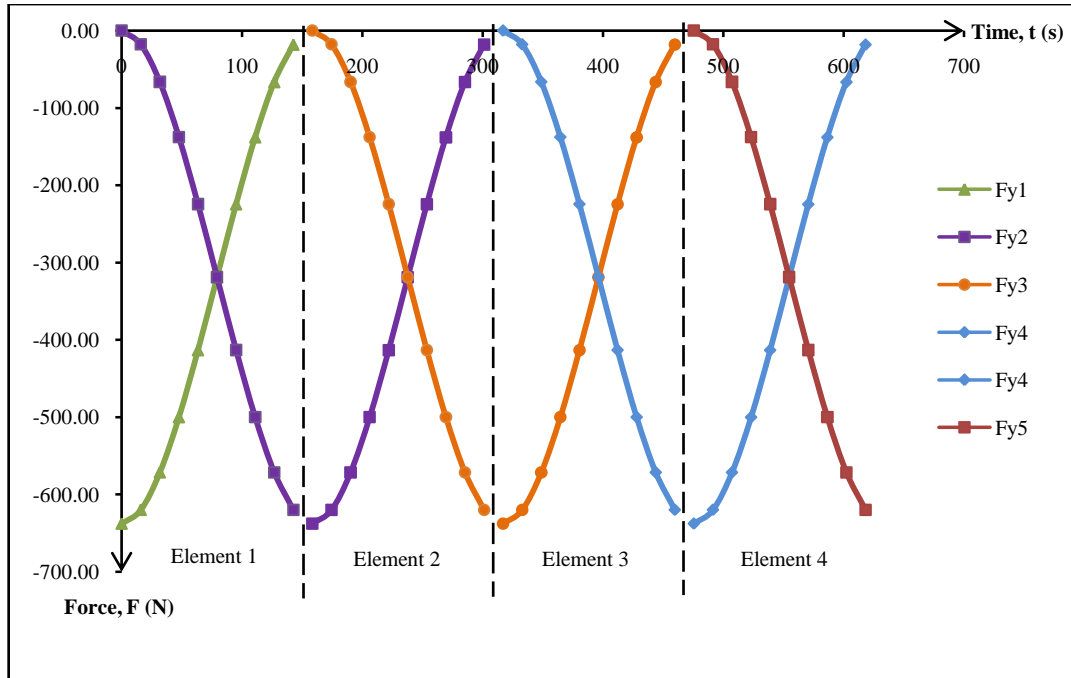
Figure B.2: Plot of Nodal force versus time

C. ANSYS Codes

C.1 Creating the 2D Beam Model in ANSYS [5]

Firstly, the Element Type and material properties need to be defined. The following is the codes which can be used if not using the graphical user interface (GUI).

```
/PREP7
ET,1,BEAM3                    ! Defining element type as "BEAM3"
R,1,0.09,1.875E-5,0.05, , , , ! Defining material properties (Cross-sectional area, Area moment of inertia, Height)
MPTEMP,,,,,,,,
MPTEMP,1,0
MPDATA,EX,1,,1.96E10          ! Defining modulus of elasticity as $1.96 \times 10^{10}$ Pa
MPDATA,PRXY,1,,0.3            ! Defining Poisson's ratio as 0.3
MPTEMP,,,,,,,,
MPTEMP,1,0
MPDATA,DENS,1,,980            ! Defining material density as 980 kg/m$^3$
mat,1
type,1
real,1
```

Since the 428m long beam is to be divided into 30 elements of equal length, there will be 31 nodes. The 31 nodes are created and labeled first.

```
*DO,i,1,11,1
N,i,(i-1)*100,0,0             ! Creating Nodes
*ENDDO
```

After that, Node 1 is joined to Node 2 to create Element 1, Node 2 to Node 3 to create Element 2 and so on. This procedure is repeated until all 30 elements were created.

```
*DO,i,1,10,1
EN,i,i,i+1                    ! Creating Elements by joining adjacent Nodes
*ENDDO
FINISH                       ! Signifies the end of Modeling process
```

C.2   Programming the Moving Single Point Load [5]

Some constants need to be defined beforehand to enable programming of the moving load. In the earlier section (Appendix Section B.2), 300 steps were needed to completely traverse across the beam. For more accurate results, the number of steps was increased to 1000 to refine the analysis.

```
Lt = 428                    ! Define beam length in m

EL = 30                     ! Define number of elements

N = EL + 1                  ! Define number of nodes

P = -637.65                 ! Forcing function in Newtons, single point force

V = 0.09                    ! Define speed of moving load in m/s

L = Lt/EL                   ! Define length of each element

ttotal = L/V                ! Total time taken for load to completely traverse entire length of beam

tstep = 1000                ! Total number of steps to completely traverse entire length of beam

deltat = ttotal/tstep       ! Time taken for one step
```

C.3 Programming the Transient Analysis Solution [5]

Once the bridge modeling and defining the constants were completed, the next step would be to setup the solution. The analysis type, boundary conditions and loads need to be defined.

```
/CONFIG,NRES,tstep

/SOL

ANTYPE,4                    ! Selecting "Transient" as Analysis Type

TRNOPT,FULL

LUMPM,0                     ! Deactivating Lumped Mass assumption

ALPHAD,0

BETAD,0.0005                ! Setting Beta damping to 0.05%


D,1, ,0, , , ,UX,UY, ROTZ, , ,    ! Defining fixed support at Node 1

                            ! zero deflection in x- and y-axes and zero rotation about z-axis

D,31, ,0, , , ,UX,UY, ROTZ, , ,   ! Defining fixed support at Node 31

                            ! zero deflection in x- and y-axes and zero rotation about z-axis


TM_START = 0.001            ! Starting time (must be > 0)

TM_END = ttotal             ! Ending time of the transient

TM_INCR=deltat              ! Time increment


*DO,TM,TM_START,TM_END,TM_INCR

        TIME,TM                     ! Time value

        *DO,i,1,31,1

                xp = V*TM           ! Determine exact location of load

                ff = (xp/L+1)/NINT(xp/L+1)

                *IF,ff,GE,1,THEN

                        s1 = NINT(xp/L)

                *ELSE

                        s1 = NINT(xp/L)-1

                *ENDIF
```

```
        s = s1+1                    ! Defines on which element the load is located

        zeta = (xp - (s-1)*L)/(L)
        N1 = 1 - 3*zeta**2 + 2*zeta**3
        N2 = (zeta - 2*zeta**2 + zeta**3)*L      } ! Calculation of shape functions
        N3 = 3*zeta**2 - 2*zeta**3
        N4 = (-zeta**2 + zeta**3)*L


        *IF,i,EQ,s,THEN
                Fy11 = P*sin(2*TM)*N1
                Mz11 = P*sin(2*TM)*N2
        *ELSEIF,i,EQ,s+1
                Fy11 = P*sin(2*TM)*N3          } ! Calculation of magnitude of force and moment
                Mz11 = P*sin(2*TM)*N4
        *ELSE
                Fy11 = 0
                Mz11 = 0
        *ENDIF


        F,i,FY,Fy11                 ! Apply force Fy11 at Node i
        F,i,MZ,Mz11                 ! Apply moment Mz11 at Node i
    *ENDDO


    SOLVE                           ! Initiate solution calculations
*ENDDO                              ! Complete calculations for entire length of beam
```